



저작자표시-비영리-변경금지 2.0 대한민국

이용자는 아래의 조건을 따르는 경우에 한하여 자유롭게

- 이 저작물을 복제, 배포, 전송, 전시, 공연 및 방송할 수 있습니다.

다음과 같은 조건을 따라야 합니다:



저작자표시. 귀하는 원저작자를 표시하여야 합니다.



비영리. 귀하는 이 저작물을 영리 목적으로 이용할 수 없습니다.



변경금지. 귀하는 이 저작물을 개작, 변형 또는 가공할 수 없습니다.

- 귀하는, 이 저작물의 재이용이나 배포의 경우, 이 저작물에 적용된 이용허락조건을 명확하게 나타내어야 합니다.
- 저작권자로부터 별도의 허가를 받으면 이러한 조건들은 적용되지 않습니다.

저작권법에 따른 이용자의 권리는 위의 내용에 의하여 영향을 받지 않습니다.

이것은 [이용허락규약\(Legal Code\)](#)을 이해하기 쉽게 요약한 것입니다.

[Disclaimer](#)

이학박사학위논문

**SAMHD1 결핍에 의한 자가면역 질환
생성 기작에 대한 연구**

**Signaling mechanisms linking *SAMHD1*-deficiency
to the type I interferonopathy**

2018 년 2 월

서울대학교 대학원

협동과정 유전공학전공

오 창 훈

CONTENTS

CONTENTS	I
LIST OF TABLES AND FIGURES	IV
LIST OF ABBREVIATIONS	VIII
ABSTRACT	1
INTRODUCTION	
1 Characteristics of SAMHD1 protein	7
2. SAMHD1-mediated retroviral restriction	
1	0
3. SAMHD1 and Aicardi-Goutières syndrome	
1	4
MATERIALS AND METHODS	

1. Generation of knockout cell lines	19
2. Cells and human blood cell isolation	21
3. Reagents and antibodies	21
4. RNA interference and transfection	22
5. Genomic DNA and RNA preparation	23
6. Quantitative real-time reverse transcription PCR	
2	3
7. Cell cycle analysis	
2	6
8. In vitro nuclease assay by immunoprecipitation	
2	6
9. CLIP-seq and RNA-seq	27
10. Bioinformatics	29
11. Ethical statement	31
12. Statistical analysis	31

RESULTS

1. <i>SAMHD1</i> -deficient human monocytic cells display a heightened IFN signature	33
2. RNA enriched in the absence of <i>SAMHD1</i> is a major source of the IFN- α response	48
3. ISG activation in <i>SAMHD1</i> -deficient cells is dependent on IRF3 & Type I IFN receptor	73
4. The PI3K/AKT signaling pathway is involved in linking <i>SAMHD1</i> -deficiency to the IFN response	81
DISCUSSION	115
REFERENCES	122
ABSTRACT IN KOREAN	129
APPENDIX	134

LIST OF TABLES AND FIGURES

Table 1. sgRNA sequence for the generation of <i>SAMHD1</i> and <i>AKT1</i> knockout c e l l l i n e s .	20
Table 2. Primer sequences used for mRNA expression.	25
Figure 1. Schematic illustration of SAMHD1 protein.	9
Figure 2. S A M H D 1 - m e d i a t e d r e s t r i c t i o n t o H I V - 1 .	2
Figure 3. Proposed mechanism of AGS pathogenesis.	16
Figure 4. Knockout of <i>SAMHD1</i> activates an immune response in human m o n o c y t i c c e l l s .	

3	4
Figure 5. Knockout of <i>SAMHD1</i> induces type I IFN production in human monocyctic cells .	
3	6
Figure 6. Differentiated THP-1 cells do not show a distinct IFN signature in <i>SAMHD1</i> -deficiency.	38
Figure 7. The effect of <i>SAMHD1</i> -deficiency on cell cycle distribution.	
3	9
Figure 8. The effect of changes in serum concentration on the manipulation of cell cycle.	40
Figure 9. The manipulation of cell cycle is not responsible for the autoimmune phenotypes in <i>SAMHD1</i> -deficient cells.	42
Figure 10. Identification of DEGs in <i>SAMHD1</i> -deficient THP-1 cells.	
4	4
Figure 11. Classification of DEGs in <i>SAMHD1</i> -deficient THP-1 cells.	
4	6
Figure 12. Bioinformatic prediction of the upstream regulators of DEGs in <i>SAMHD1</i> -deficient THP-1 cells.	49
Figure 13. IFN signature in <i>SAMHD1</i> -deficient THP-1 cells.	
5	1

Figure 14. Verification of IFN signature in <i>SAMHD1</i> -deficient THP-1 cells.	
5	3
Figure 15. Accumulated RNAs in <i>SAMHD1</i> -deficient cells function as immune stimuli.	
	54
Figure 16. Large RNAs in <i>SAMHD1</i> -deficient cells function as immune stimuli.	
	57
Figure 17. Cytoplasmic RNA from <i>SAMHD1</i> -deficient cells activates a type I IFN response.	
5	9
Figure 18. RNA from PMA-differentiated <i>SAMHD1</i> -deficient cells do not induce distinct <i>IFN-α</i> expression.	
6	1
Figure 19. RNA from <i>SAMHD1</i> -deficient cells activates a type I IFN response.	
	64
Figure 20. <i>SAMHD1</i> protein immunopurified from undifferentiated THP-1 cells possesses RNase activity.	
	66
Figure 21. RNase activity of <i>SAMHD1</i> is involved in the regulation of IFN response.	
	69
Figure 22. <i>SAMHD1</i> CLIP-seq.	
	71
Figure 23. Depletion of nucleic acid sensors or downstream molecules using	

siRNA treatment.	74
Figure 24. IRF3 is indispensable for ISGs induction in <i>SAMHD1</i> -deficiency.	
7	6
Figure 25. Secreted proteins from <i>SAMHD1</i> -deficient cells elevate ISG levels in a time-dependent manner.	
7	9
Figure 26. ISGs induction in <i>SAMHD1</i> -deficiency occurs through type I IFN receptor signaling pathway.	
8	2
Figure 27. JAK inhibitor treatment diminishes ISG induction.	
8	4
Figure 28. AKT is highly activated in <i>SAMHD1</i> -deficient cells.	
8	6
Figure 29. PI3K inhibitor blocks the induction of type I IFN and ISGs.	
8	9
Figure 30. PI3K inhibitor suppresses the activation of STAT1 and AKT.	
9	1
Figure 31. AKT inhibitor diminishes the induction of type I IFN and ISGs.	
9	3
Figure 32. AKT inhibitor abolishes the activation of STAT1 and AKT.	

9	5
Figure 33. <i>AKT</i> knockout abrogates the activation of IRF3 and STAT1 in <i>SAMHD1</i> -deficient cells.	97
Figure 34. <i>AKT</i> knockout abrogates <i>SAMHD1</i> -associated AGS phenotypes.	
9	9
Figure 35. The PI3K/AKT functions upstream of type I IFN receptor signaling pathway	102
Figure 36. The PI3K/AKT functions upstream of IRF3 to activate type I IFN response	104
Figure 37. RNase activity of <i>SAMHD1</i> is responsible for the activation of <i>AKT</i> .	106
Figure 38. siRNA-mediated <i>SAMHD1</i> silencing in human PBMCs recapitulates the phenotypes seen in <i>SAMHD1</i> -deficient THP-1 cells.	109
Figure 39. <i>SAMHD1</i> -deficient 293T cells do not display AGS phenotypes.	111
Figure 40. <i>SAMHD1</i> -deficient HeLa cells do not display AGS phenotypes.	113
Figure 41. A working model for <i>SAMHD1</i> -related interferonopathy in AGS.	117

LIST OF ABBREVIATIONS

SAMHD1	sterile alpha motif domain and HD domain-containing protein 1
dNTPase	deoxynucleoside triphosphohydrolase
NLS	nuclear localization signal
ISGs	IFN-stimulated genes
CRISPR	clustered regularly interspaced short palindromic repeats
RT	reverse transcriptases
HIV	human immunodeficiency virus
AGS	Aicardi-Goutières syndrome
SLE	systemic lupus erythematosus

IFN	interferon
sgRNA	single guide RNAs
TNF- α	tumor necrosis factor alpha
NF- κ B	nuclear factor-kappa B
ELISA	enzyme-linked immunosorbent assay
RNA-seq	RNA sequencing
qRT-PCR	quantitative real-time reverse transcription polymerase chain reaction
PMA	phorbol 12-myristate 13-acetate
RIG-I	retinoic acid-inducible gene-I
MDA5	melanoma differentiation associated gene 5
HITS-CLIP	high-throughput sequencing of RNA isolated by crosslinking immunoprecipitation
RLR	RIG-I-like receptor
TLR	Toll-like receptor
siRNA	short interfering RNA
IRF3	Interferon Regulatory Factor 3
JAK	Janus activated kinase
STAT	signal transducers and activators of transcription

ERK	extracellular signal-regulated kinase
PI3K	phosphoinositide 3-kinase
Cas9	CRISPR associated protein9
PBMC	peripheral blood mononuclear cell
snoRNA	small nucleolar RNA

ABSTRACT

Signaling mechanisms linking *SAMHD1*-deficiency to the type I interferonopathy

Changhoon Oh
Department of Interdisciplinary Program
in Genetic Engineering
The Graduate School
Seoul National University

SAMHD1 is an enzyme which has dual enzymatic activities: deoxynucleoside triphosphohydrolase (dNTPase) and phosphorolytic 3'-5' exoribonuclease. Even though *SAMHD1* was identified initially as the human ortholog of the mouse IFN γ -induced gene *Mg11*, studies about *SAMHD1* have focused overwhelmingly on the inhibitory mechanism of *SAMHD1* against HIV-1 replication. *SAMHD1* was demonstrated to restrict HIV-1 replication by reducing cellular dNTP concentrations below the levels required for retroviral reverse transcription in dNTPase dependent manner. In addition, it is also suggested that *SAMHD1* can bind to and degrade HIV-1 RNA to restrict the replication of HIV-1 through the RNase activity.

A disturbance of the type I interferon homeostasis is central to the pathogenesis of the autoimmune diseases. The autoimmune disorder Aicardi-Goutières syndrome (AGS) is characterized by a constitutive type I interferon

response clinically overlapping with congenital infection and systemic lupus erythematosus (SLE). All the genes that are mutated in patients with AGS encode enzymes (TREX1, RNASEH2, ADAR, SAMHD and IFIH1) that are associated with nucleic acid metabolism, leading to the hypothesis that the inappropriate accumulation of endogenous nucleic acid species resulting from the dysfunction of AGS-related enzymes triggers the chronic type I interferon response. The mechanisms by which malfunctions of TREX1, RNASEH2, ADAR1 and IFIH1 occur AGS are considerably investigated and suggested. However, how *SAMHD1*-deficiency causes the type I interferon response in patients with AGS remains unknown, even though mutations in *SAMHD1* cause AGS. In addition, *Samhd1*-deficient mice did not exhibit any distinct clinical phenotypes. Therefore, it is very important to identify the mechanism by which *SAMHD1*-deficiency results in AGS in human patients.

Here, I generated *SAMHD1*-deficient THP-1 cell lines and showed that those cell lines recapitulate AGS phenotypes which include the activation of type I interferon response and delayed cell cycle progression. I further showed that SAMHD1 proteins purified from undifferentiated THP-1 cells possessed RNase activity. Then, RNA derived from *SAMHD1*-deficient cells, but not that from wild-type cells neither DNA derived from wild-type and *SAMHD1*-deficient cells, significantly activated *IFN- α* expression. In addition, the reconstitution of wild-

type SAMHD1 and SAMHD1_{D137N}, which possess RNase activity, only repressed the *IFN- α* induction in *SAMHD1*-deficient cells. These results suggest that cytosolic RNA species accumulated in the absence of SAMHD1 act as a major immunogenic source for the type I interferon response. I also proposed that innate sensing of the endogenous retroelements-derived transcripts accumulated in *SAMHD1*-deficient cells results in significant type I interferon response and this accounts for the cause of SAMHD1-related AGS. This was supported with my data showing significant portion of the retroelement RNAs identified in *SAMHD1* CLIP-seq and upregulated in *SAMHD1*-deficient cells. Even though many nucleic acid sensing pathways were already identified, this IFN signature occurred independently of all previously known nucleic acid sensing pathways that ultimately converge on activation of TBK1. Only IRF3 was indispensable for the spontaneous IFN signature in *SAMHD1*-deficient cells. Therefore, I sought to identify the RNA sensing pathway associated with ISG induction in *SAMHD1*-deficient cells and showed that the PI3K/AKT/IRF3 signaling pathway is essential for the type I interferon response in *SAMHD1*-deficient THP-1 cells. AKT and IRF3 were highly activated in *SAMHD1*-deficient cells, as assessed by the phosphorylation levels of these molecules. Then, treatment of PI3K or AKT inhibitors dramatically reduced the type I interferon signatures in *SAMHD1*-

deficient cells. Moreover, *SAMHD1/AKT1* double knockout relieved the type I interferon signatures to the levels observed in wild-type cells. The reconstitution of wild-type *SAMHD1* and *SAMHD1*_{D137N} inhibited the activation of AKT in *SAMHD1*-deficient cells, showing that RNase activity of *SAMHD1* is critical for AKT activation as well as spontaneous IFN response. In human PBMCs, siRNA-mediated *SAMHD1* silencing recapitulated the phenotypes seen in *SAMHD1*-deficient THP-1 cells. By comparison, knockout of *SAMHD1* in not only HEK293T and HeLa cells but also PMA-differentiated THP-1 cells did not result in the activation of STAT1 or the induction of ISGs, suggesting that the type I interferonopathy associated with *SAMHD1*-deficiency is cell type-specific. My data provide an insight not only into the pathogenesis of the type I interferonopathies but also will encourage the development and use of immunosuppressive therapies in AGS and related autoimmune diseases.

Keyword: AGS, *SAMHD1*, RNase, PI3K, AKT, IRF3, interferonopathy

Student number: 2009-30842

INTRODUCTION

1. Characteristics of SAMHD1 protein

SAMHD1 is an antiviral protein that is highly expressed in cells of the myeloid lineage (1, 2). SAMHD1 was identified initially as the human ortholog of the IFN γ -induced gene Mg11 (3). SAMHD1 consists of N-terminal sterile alpha motif (SAM) domain and C-terminal HD domain. Of the two domains, the former is expected to be involved in protein-protein or protein-RNA interaction (4). The latter is a characteristic of an enzyme family with phosphodiesterase or nuclease activity (5). The experiments using purified recombinant SAMHD1 proteins demonstrated that SAMHD1 has dGTP-activated deoxynucleoside triphosphohydrolase (dNTPase) activity which cleaves the triphosphate from deoxynucleoside triphosphate (6-8). Recently, it has been reported that dNTPase activity of SAMHD1 is affected by the phosphorylation or the acetylation status of SAMHD1 (9-11). Moreover, phosphorolytic 3'-5' exoribonuclease activity of SAMHD1 that degrades single-stranded RNA was also identified (12, 13).

The wild-type SAMHD1 is mainly detected in the nucleus, because SAMHD1 possesses a classical nuclear localization signal (NLS) (14, 15). However, SAMHD1 is also found in the cytoplasm (16) and the mutagenesis of NLS

causes the change in the cellular localization of SAMHD1 from the nucleus to the cytoplasm.

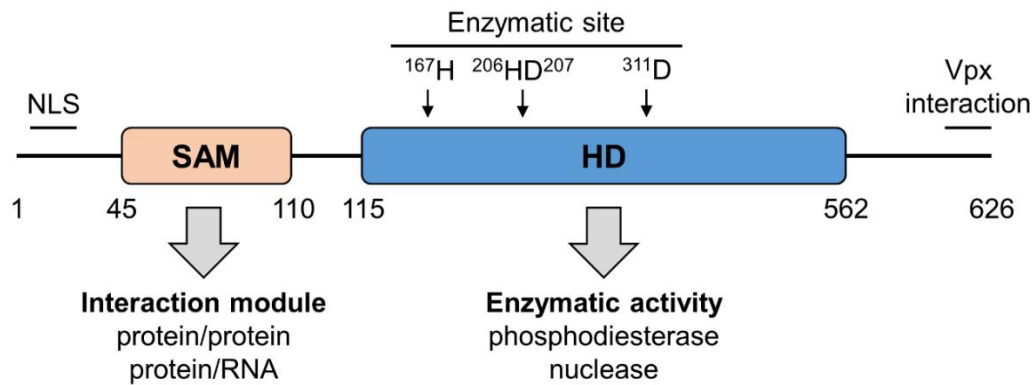


Figure 1. Schematic illustration of SAMHD1 protein and its functional domains

SAMHD1 is a 626 amino acid protein which has an SAM and HD domain. NLS located in N-terminus, a critical region which is responsible for Vps interaction and four residues in HD domain are indicated. Numbers denote the position of amino acids in SAMHD1 protein.

2. SAMHD1-mediated retroviral restriction

The concentration of dNTP pools in mammalian cells are tightly regulated and differ depending on cell types, differentiation state and cell cycle (17). It is known that intracellular nucleotides can control retroviral infections through the regulation of DNA synthesis by reverse transcriptases (RT) (18). Even though lentiviral RTs such as HIV-1 and SIV can be functional at the low dNTP concentrations compared with retroviral RTs (19, 20), HIV-1 can rarely infect quiescent cells that have severely decreased dNTP pools (7, 21). It is also indicated that the Vpx, an accessory protein of SIV and HIV-2, mediated degradation of SAMHD1 can enhance the infectivity of HIV-1 in human DCs and macrophages (1, 2, 22, 23). These results led to the hypothesis that SAMHD1 suppresses HIV-1 replication by depleting the intracellular dNTP pools. Many studies demonstrated that SAMHD1 lowers the concentration of intracellular dNTPs below the levels to support reverse transcription (1, 2, 6, 7, 24, 25). On the contrary, Vpx-mediated SAMHD1 degradation significantly increased dNTP concentration and Vpx counteracted the SAMHD1-mediated HIV-1 restriction in myeloid cells (26). These studies indicate the strong inverse correlation between SAMHD1 expression and dNTP concentration/HIV-1

replication. However, the addition of dN into resting CD4+ T cells could not completely restore HIV-1 infectivity, even though it significantly increased the intracellular dNTP concentration (16). Furthermore, the phosphorylation of SAMHD1 at Thr-592 negatively regulated the HIV-1 restriction function of SAMHD1 without any changes in the cellular dNTP levels (27, 28). Thus, it is suggested that an additional cellular function of SAMHD1 may be involved in SAMHD1-mediated HIV-1 restriction.

Recent studies reported that SAMHD1 functions as a 3'-5' exonuclease degrading ssRNA or ssDNA in vitro (12, 29). Those also demonstrated that SAMHD1 can bind to and degrade HIV-1 RNA, suggesting the novel mechanism of SAMHD1 restricting the replication of HIV-1 and retroviruses. However, several studies reported that they did not observe the RNase activity of SAMHD1 in vitro (30, 31), thus the existence of RNase activity of SAMHD1 is still controversial.

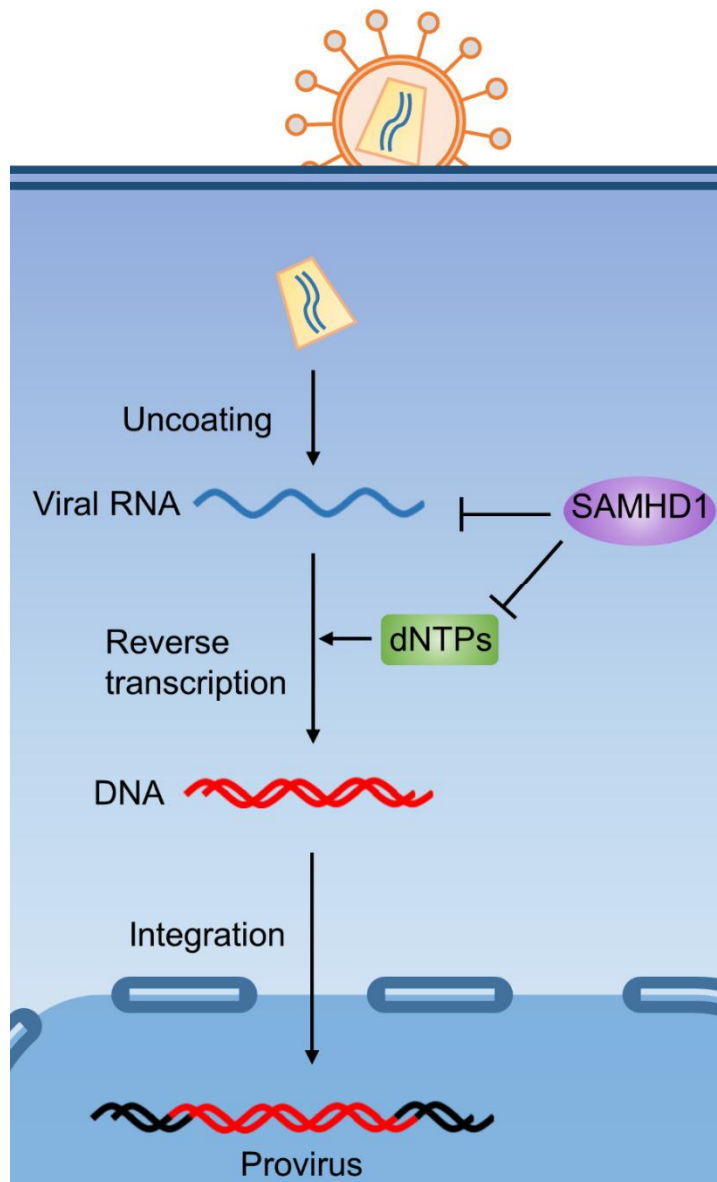


Figure 2. SAMHD1-mediated restriction to HIV-1

After viral entry, viral genomic RNA is released into the cytoplasm and reverse transcribed in a linear dsDNA. SAMHD1 possesses both dNTPase and RNase activity. SAMHD1 can function as a dNTPase to decrease the levels of DNA building block, dNTPs and subsequently inhibit the reverse transcription of HIV-1. In addition, SAMHD1 can directly bind and degrade HIV-1 genomic RNA to restrict the replication of HIV-1.

3. SAMHD1 and Aicardi-Goutières syndrome

Although studies have focused overwhelmingly on the inhibitory mechanism of SAMHD1 against HIV-1 replication because of an unexpected identification of SAMHD1 as an HIV-1 restriction factor, SAMHD1 has been proposed to serve as a negative regulator of the innate immune response (32). It has been reported that mutations in SAMHD1 gene are associated with Aicardi-Goutières syndrome (AGS). AGS is a monogenic autoinflammatory disorder that overlaps phenotypically with congenital viral infection and systemic lupus erythematosus (SLE), and is characterized by constitutive upregulation of type I interferon (IFN) in the serum and cerebrospinal fluid (33). Some children with AGS also display an early onset form of SLE. While SLE is associated with more than 20 genes, AGS is caused by autosomal recessive mutations in one of several genes encoding enzymes involved in nucleic acid metabolism (TREX1, RNASEH2, ADAR and SAMHD1) or by gain-of-function mutations in the cytosolic RNA sensor IFIH1 (32, 34-38). Given that the pathology of SLE is complex and heterogeneous, AGS could be an excellent model disease to study systemic autoimmunity and provide a clue to the pathogenesis of SLE. Considering that all of the AGS-related genes associated with nucleic acid

metabolism and nucleic acid sensing dysfunction implicated in autoimmunity, the elevated IFN signature observed in SAMHD1-related AGS patients might be caused by activation of the innate immune response against dysregulated endogenous nucleic acids. Even though SAMHD1 possesses dual enzymatic activities, the physiological function of SAMHD1 under natural conditions remains poorly understood. Therefore, the mechanism by which the mutations in SAMHD1 cause AGS needs to be revealed.

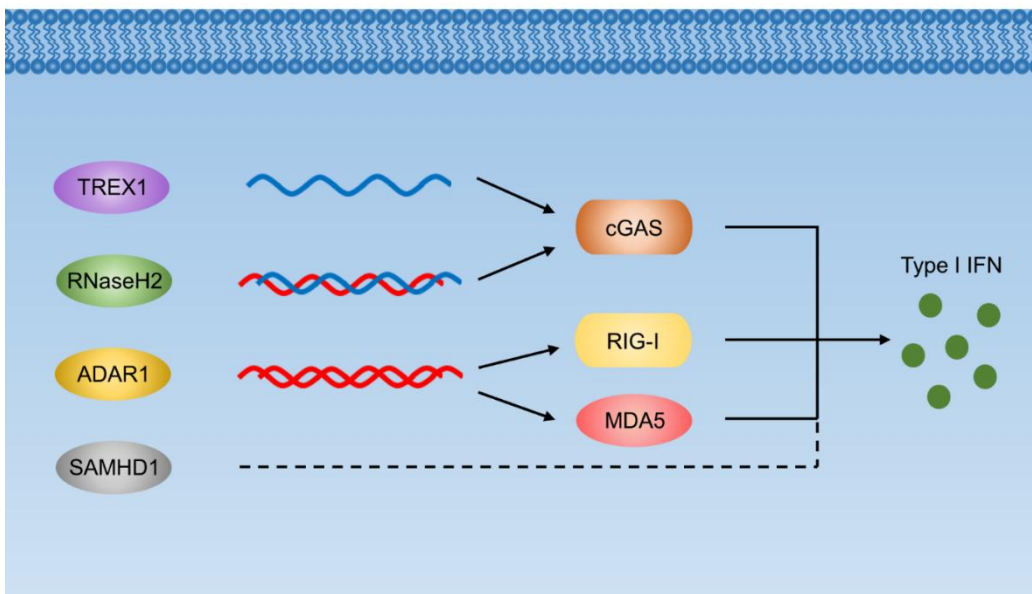


Figure 3. Proposed mechanism of AGS pathogenesis

Lack of Trex1 or RNaseH2 activity induces the accumulation of ssDNA or RNA:DNA hybrids in cytoplasm, respectively. The augmented pool of DNA or RNA: DNA hybrids in cytoplasm leads to the activation of nucleic acid sensor cGAS. The defect of RNA editing by ADAR1 induces aberrant IFN response to dsRNA in RIG-I and MDA5 dependent manner. The mutant MDA5 lacked RNA-specific responsiveness also increase type I IFN response by itself. SAMHD1 is proposed to affect the amount of dNTP for DNA synthesis and impair nucleic acid homeostasis. However, it is not clearly identified.

MATERIALS AND METHODS

1. Generation of knockout cell lines

Wild-type and mutants of SAMHD1 were amplified by PCR from previously described plasmids (12) and inserted into the EGFP-N3 vector. SAMHD1-deficient THP-1, HEK239T and HeLa cells were generated using the CRISPR/Cas9 system. The SAMHD1/AKT double knockout THP-1 cell line was established by transfecting SAMHD1-deficient THP-1 cells with single guide RNAs (sgRNAs) specific for AKT1. Immunoblotting and genomic DNA sequencing confirmed all the knockout cell lines. Guide RNA sequences of SAMHD1 and AKT1 are listed in Table 1.

Table 1. sgRNA sequence for the generation of *SAMHD1* and *AKT1* knockout cell lines

sgRNA sequence	
Genomic Target	Target site sequence
SAMHD1-1	CTCAAACACCCCTTCCGCAG
SAMHD1-2	GGCAGACTGGTCCCCGGGCC
AKT1-1	GCAGGATGTGGACCAACGTG
AKT1-2	TGTTGAGGGGAGCCTCACGT

2. Cells and human blood cell isolation

THP-1 was cultured in Roswell Park Memorial Institute (RPMI) 1640 supplemented with 10 % fetal bovine serum (FBS), 2 mM GlutaMAX-I, and 1 % penicillin/streptomycin. 293T cells were maintained in Dulbecco's modified Eagle's medium (DMEM) supplemented with 10 % FBS, 2 mM GlutaMAX-I, and 1 % penicillin/streptomycin. PBMCs were isolated from human blood of healthy donors using SepMate, according to the manufacturer's instruction (Stemcell). Isolated PBMCs were transfected with SAMHD1 specific siRNA or control non-specific siRNA for two cycles to obtain efficient knockdown and incubated in RPMI media. After 48 h of incubation, PBMCs were analyzed by western blotting analysis to monitor the activation of STAT1 and AKT.

3. Reagents and antibodies

The chemical reagents and antibodies used in this study were purchased from the following manufacturers: poly (I:C) and poly (dA:dT), Sigma; T4 Polynucleotide Kinase and T4 RNA ligase, Takara; T4 RNA Ligase 2 (truncated K227Q) and Antarctic Phosphatase, New England Biolabs (NEB); wortmannin

and rapamycin, Sigma; MK-2206, A-674563, and Lapatinib, Selleckchem; Ruxolitinib, Invivogen; mouse monoclonal antibodies to IFNAR1 (Millipore) and SAMHD1 (OriGene); rabbit monoclonal antibodies to IRF3 pho-S386 (Abcam), RIG-I, STING, MyD88, TBK1, TBK1 pho-S172, Stat1 pho-Y701, and GSK-3 β (all from Cell Signaling Technology); rabbit polyclonal antibodies to IRF3 (Santa Cruz), SAMHD1 (for immunoprecipitation, Bethyl Lab), GAPDH (Ab Frontier), MAVS, TRIF, IRF7, STAT1, Akt, Akt pho-S473, and GSK-3 β pho-S9 (all from Cell Signaling Technology); goat polyclonal antibody to hIL-10Rb (R&D systems)

4. RNA interference and transfection

All siRNAs were purchased from Dharmacon as ON-Target plus. THP-1 cells were transfected by electroporation with indicated gene-specific siRNAs or non-specific siRNAs using Neon (Invitrogen). Lysates were collected 72 h after transfection for western blotting and qRT-PCR analysis. For nucleic acid stimulation, PMA-differentiated THP-1 cells were transfected with 5 μ g/ml of poly (I:C), poly (dA:dT), or isolated DNA or RNA, using Lipofectamine 2000 transfection reagent (Invitrogen) and undifferentiated THP-1 cells were

transfected by electroporation with 10 µg/ml of isolated RNA using Neon. Cells were harvested 4 h post transfection, followed by RNA isolation. For reconstitution of SAMHD1-deficient THP-1, THP-1 cells were transfected by electroporation with expression vectors for wild-type or mutant SAMHD1 using Neon. Isolated PBMCs were transfected using Interferin™ transfection reagent (Polyplus-transfection Inc.), according to the manufacturer's instructions.

5. Genomic DNA and RNA preparation

Genomic DNA was purified using a Blood Mini Kit (Qiagen). Total RNA was isolated using the TRIzol reagent (Invitrogen). Fractionation and extraction of small and large RNAs were performed using the NucleoSpin miRNA system (Macherey-Nagel). Separation and purification of cytoplasmic and nuclear RNAs were carried out using a Cytoplasmic & Nuclear RNA purification kit (Norgen). All the purification steps were processed according to the manufacturers' instructions.

6. Quantitative real-time reverse transcription PCR

Total RNA was subjected to cDNA synthesis using the ReverTra Ace qPCR RT Kit (TOYOBO), according to the manufacturer's instructions. The expression levels of various genes were measured using the iCycler iQ real-time PCR detection system (BioRad) using the TOPreal qPCR PreMIX (Enzynomics). The data were normalized to the expression level of β -actin or GAPDH. The primer sets used are listed in Table 2.

Table 2. Primer sequences used for mRNA expression

mRNA expression primer sequences	
Gene Product	Sequences
β -actin Forward	CATGTACGTTGCTATCCAGGC
β -actin Reverse	CTCCTTAATGTCACGCACGAT
GAPDH Forward	ACCCAGAAGACTGTGGATGG
GAPDH Reverse	GGTCCTCAGTGTAGCCCAAG
IFNA4 Forward	ACCTGGTTCAACATGGAAATG
IFNA4 Reverse	ACCAAGCTTCTTCACACTGCT
IFN β Forward	AGTAGGCGACACTGTTTCGTG
IFN β Reverse	GCCTCCCATTC AATTGCCAC
IFITM1 Forward	CCCCCAGCACCATCCTTC
IFITM1 Reverse	ACCCCGTTTTTCCTGTATTATCTGT
MxA Forward	AGGTCAGTTACCAGGACTAC
MxA Reverse	ATGGCATTCTGGGCTTTATT
ISG15 Forward	ACTCATCTTTGCCAGTACAGGAG
ISG15 Reverse	CAGCATCTTCACCGTCAGGTC
IFIT1 Forward	GCAGCCAAGTTTTACCGAAG
IFIT1 Reverse	GCCCTATCTGGTGATGCAGT
IFIT2 Forward	CGAACAGCTGAGAATTGCAC
IFIT2 Reverse	CAAGTTCAGGTGAAATGGC
IFIT3 Forward	AGTCTAGTCACTTGGGGAAAC
IFIT3 Reverse	ATAAATCTGAGCATCTGAGAGTC
IFI27 Forward	GGCAGCCTTGTGGCTACTCT
IFI27 Reverse	ATGGAGCCCAGGATGAACTTG
IFI44L Forward	GTATAGCATATGTGGCCTTGCTTACT
IFI44L Reverse	ATGACCCGGCTTTGAGAAGTC
RSAD2 Forward	AGGTTCTGCAAAGTAGAGTTGC
RSAD2 Reverse	GATCAGGCTTCCATTGCTC

7. Cell cycle analysis

Wild-type or SAMHD1-deficient THP-1 cells were incubated in varying serum concentration. After 48 h, cells were harvested and washed twice with PBS. Then the cells were fixed with 70% cold ethanol overnight at 4°C, followed by washing twice with PBS. The cells were then resuspended with 0.5 ml PBS and 5 µl of 20 mg/ml RNase A and 10 µl of 1 mg/ml PI solution were added, followed by analysis on BD FACSCanto II (BD Biosciences)

8. *In vitro* nuclease assay by immunoprecipitation

Pelleted THP-1 cells were lysed for 30 min at 4 °C in lysis buffer (25 mM Tris-HCl, pH 7.5, 100 mM KCl, 1 mM DTT, 2 mM EDTA, 0.5 mM PMSF, 0.05 % NP-40, RNase inhibitor). After sonication, the lysates were centrifuged for 30 min at 13,000 × g at 4 °C. anti-SAMHD1 and anti-rabbit IgG antibodies were incubated with Dynabeads for 1 h at room temperature. The conjugated beads were washed sequentially twice each with buffer A (500 mM NaCl, 10 mM Tris-HCl, pH 7.5, 0.05 % NP-40, RNase inhibitor) and buffer B (150 mM NaCl, 10 mM Tris-HCl, pH 7.5, 0.05 % NP-40, RNase inhibitor). Cell lysates were

incubated with the prepared conjugated Dynabeads for 1 h at 4 °C. The immunoprecipitates were washed five times with buffer B, followed by an in vitro nuclease assay. The in vitro nuclease assay was performed as described previously (12). In brief, immunoprecipitated proteins were incubated in 20 µl reaction mixtures containing phosphate-buffered saline (PBS) supplemented with 5 mM MgCl₂, 2 mM dithiothreitol (DTT) and [γ-³²P]-labeled RNA substrate (A20) at 37 °C for 30 min. The reactions were stopped by the addition of 20 µl of 2× RNA loading buffer and then boiled at 95 °C for 5 min. RNA was separated on 8 M urea/15 % polyacrylamide gels and analyzed using a BAS-2500 phosphorimager (Fujifilm).

9. CLIP-seq and RNA-seq

CLIP-seq and RNA-seq was performed as previously described (39), with some modifications. Briefly, THP-1 cells were irradiated by 254nm UV at total 600 mJ/cm² for RNA-protein cross-linking (Spectroliner) for SAMHD1-CLIP. The RNAs bound to SAMHD1 were immunoprecipitated with anti-SAMHD1 conjugated beads. After ligation with 3' adaptors (5'/rApp/TGGAATTCTCGGGTGCCAAG G/ddC/-3', Integrated DNA

Technologies) using T4 RNA Ligase 2, truncated K227Q (NEB), RNAs were labeled with [γ -³²P]ATP by T4 polynucleotide kinase (Takara). The RNA-protein complex was separated by SDS-PAGE electrophoresis, then transferred onto nitrocellulose membrane (Whatman). The membrane with RNAs was cut by a razor and RNAs were extracted by phenol/chloroform (Ambion), followed by ethanol precipitation for RNA isolation. 5' adaptors (5'-GrGrUrUrCrArGrArGrUrUrCrUrArCrArGrUrCrCrGrArCrGrA rUrC-3', Integrated DNA Technologies) were ligated using T4 RNA ligase (Takara). For RNA-seq, total RNA was extracted from wild-type and SAMHD1-deficient THP-1 cells using the TRIzol reagent (Invitrogen), according to the manufacturer's instructions. Ribosomal RNA was removed from the total RNA using a Ribo-Zero rRNA removal Kit (Epicentre). After RNA fragmentation by RNA fragmentation reagents (Ambion), RNAs of 30–60 nucleotides were purified and ligated with 3' and 5' adaptors using T4 RNA Ligase 2, truncated K227Q, and T4 RNA ligase, respectively. 5' and 3' adaptor ligated RNAs were reverse transcribed by using the RNA RT primer (RTP; 5'-GCCTTGGCACCCGAG AATTCCA-3', Integrated DNA Technologies). PCR was performed to generate libraries for high throughput sequencing with the 5' end Illumina RNA PCR Primer (RP1) and the 3' end Illumina RNA PCR Primer with index sequences (Index 1 – 9). Sequencing was performed on a HiSeq 2000/2500 (Illumina).

10. Bioinformatics

For preprocessing, I removed adapter sequences and low-quality ends from CLIP-seq and RNA-seq reads by using Cutadapt version 1.10 with `-m 17 --match-read-wildcards -O 10 -e 0.1 -q 30,30 -g AATGATACGGCGACCAACCGA GATCTACACGTTTCAGAGTTCTACAGTCCGACGATC -a TGGAATTCTCGGGT GCCAAGGAACTCCAGTCAC` options. Artifact reads were eliminated by the `fastx_artifacts_filter` command in FASTX-Toolkit (http://hannonlab.cshl.edu/fastx_toolkit/) version 0.0.13.2. I also discarded reads mapped to human rRNA or tRNA by Bowtie2 version 2.2.7 with `-t -k 2 --very-sensitive` options. Tophat version 2.1.1 with `--no-coverage-search --b2-very-sensitive (--b2-score-min L, -0.6, -0.9 only for CLIP-seq due to the high error rate)` options was used to align these preprocessed sequencing reads against the human reference genome (GRCh37.p13) downloaded from the Reference Sequence (RefSeq) collection. In this alignment process, I also considered repetitive elements defined by the output of RepeatMasker that was downloadable from RefSeq. Based on these alignments, I calculated the read counts for each genomic position by using in-house software that

uniformly divided each multi-mapped read to all of the positions it maps to. As previously described (39), I applied Fisher's exact test to detect significant peaks (CLIP-seq enriched regions over RNA-seq). One modification in this study was that I calculated p-values for every genomic position in the whole genome background. Then, the p-values were adjusted by qvalue package in R.

RSEM (40) version 1.2.30 was used to align sequencing reads against all transcripts of the human reference genome (GRCh37.p13) downloaded from the Reference Sequence (RefSeq) collection and estimate gene-level transcript abundances. DEGs were assessed by limma package in R (41). I first filtered genes with total read counts less than 12 for 6 samples (i.e., 3 replicates of wild-type and 3 replicates of SAMHD1 knockout cells). I applied trimmed mean of M values (TMM) normalization to read counts for the estimation of scale factors among samples. Then, the voom transformation was applied to the filtered and normalized counts. After this, the usual limma procedure for differential expression analysis was followed. That is, I estimated the fold changes and standard errors by fitting a linear model for each gene and applied empirical Bayes smoothing to the standard errors. Finally, moderated t-statistics and corresponding p-values were computed. Benjamini-Hochberg method was used to adjust p-values for multiple testing.

11. Ethical statement

Human blood samples were anonymously provided by the Blood Center of the Korean Red Cross, Seoul, under the approval of the Institutional Review Board of Korean Red Cross with consent for research use. Experiments involving human blood were approved by the Institutional Review Board at Seoul National University (SNUIRB No. E1512/001-004). All experiments were performed in accordance with Seoul National University guidelines.

12. Statistical analysis

Statistical analyses were carried out using GraphPad Prism version 5.0 software. Statistical significance was determined by two-tailed Student's t-tests (* $p \leq 0.05$, ** $p \leq 0.01$, *** $p \leq 0.001$, ns: not significant)

RESULTS

1. *SAMHD1*-deficient human monocytic cells display a heightened IFN signature

AGS is a type of systemic inflammatory disease that has a type I IFN signature in human. However, *Samhd1*-deficient mice displayed neither significant upregulation of IFN-stimulated genes (ISGs) in their sera nor other systemic autoimmune phenotypes, although *Samhd1*^{-/-} mouse cells exhibited spontaneous induction of ISGs (42, 43). Therefore, I used human THP-1 cells, a well-established model of human monocytes, to study the molecular pathology of the *SAMHD1*-related AGS. I analyzed transcriptional signature of AGS using two independent *SAMHD1*-deficient THP-1 cells engineered by different clustered regularly interspaced short palindromic repeats (CRISPR) single guide RNAs (sgRNAs). Type I interferons including various subtypes of *IFN-α* and *IFN-β*, and ISGs (*IFITM1*, *CXCL10*, *OASL* and *MxA*) were upregulated in *SAMHD1*-deficient cells (Figure 4A and 4B), which was largely consistent with the results obtained from the samples of patients with AGS (44). Notably, the level of tumor necrosis factor alpha (TNF-α) was similar between *SAMHD1*-deficient and wild-type cells (Figure 4A), suggesting that *SAMHD1* is not involved in the nuclear factor-kappa B (NF-κB) pathway. The transcriptional induction of type I IFNs resulted in increased synthesis of type I IFN proteins in *SAMHD1*-deficient cells, as assessed by enzyme-linked immunosorbent assays (ELISAs) (Figure 5). To investigate the effect of the

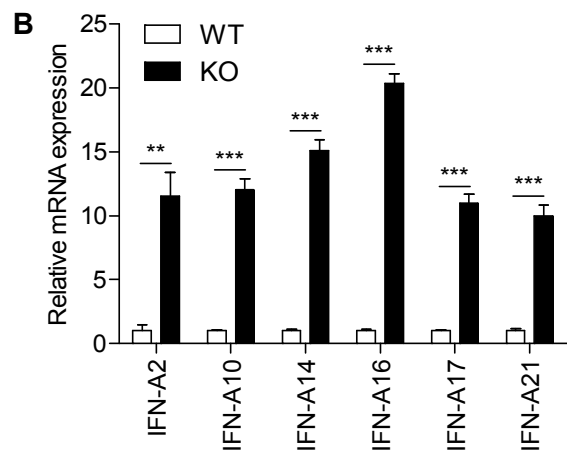
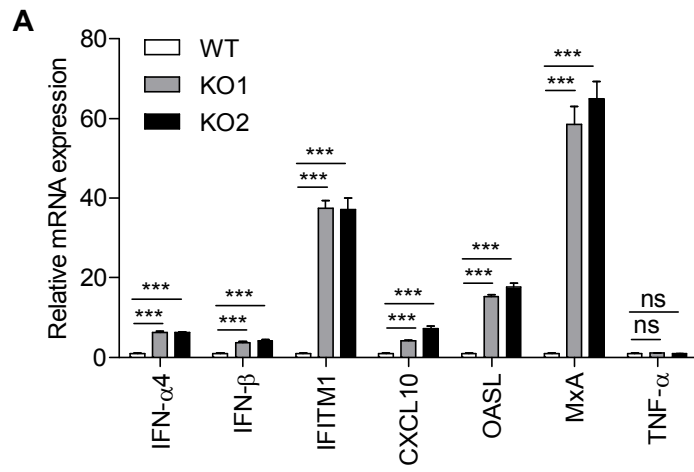


Figure 4. Knockout of *SAMHD1* activates an immune response in human monocytic cells

(A, B) Relative mRNA levels for the indicated genes in wild-type and *SAMHD1*-deficient cells, as assessed by qRT-PCR and normalized to *β-actin* expression.

In A and B, data represent the mean ± SEM of triplicate independent experiments (**p ≤ 0.01, ***p ≤ 0.001, ns: not significant, two-tailed Student's t-test).

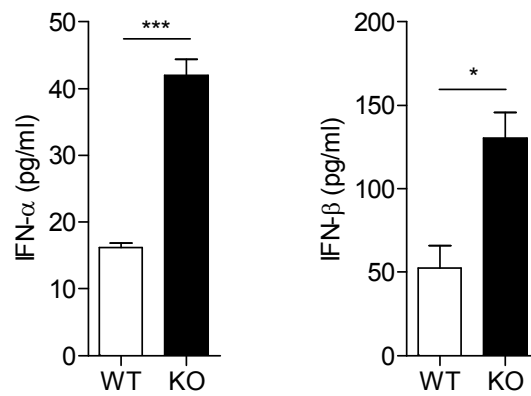


Figure 5. Knockout of *SAMHD1* induces type I IFN production in human monocytic cells

ELISA of IFN- α production in cell extracts. ELISA of IFN- β production in supernatants. Conditioned media were concentrated using Amicon Ultra-15 before analysis.

differentiation of THP-1 cells on the type I IFN signaling in *SAMHD1*-deficiency, I compared the expressions of type I IFN and ISGs in phorbol 12-myristate 13-acetate (PMA)-differentiated *SAMHD1*-deficient cells to those in PMA-differentiated wild-type cells (Figure 6). Interestingly, differentiated THP-1 cells did not show a distinct IFN signature in spite of *SAMHD1*-deficiency, proposing that *SAMHD1* related type I IFN response would be differentially displayed in cell type specific manner. Primary fibroblasts from *SAMHD1*-related AGS patients exhibited reduced proliferation and a delay in cell cycle progression (45). In agreement with this observation, *SAMHD1*-deficient THP-1 cells also displayed delayed cell cycle progression (Figure 7). To assess the relation of type I IFN response with a delayed cell cycle progression in *SAMHD1*-deficient cells, I regulated the cell cycle progression by alternating the serum concentration in culture media (46) (Figure 8). Low serum conditioning could not induce a distinct IFN signature in both wild-type and *SAMHD1*-deficient cells (Figure 9), suggesting that cell cycle delay do not explain the autoimmune phenotypes in *SAMHD1*-deficient cells.

I then performed RNA sequencing (RNA-seq) to ascertain the IFN signatures of AGS. *SAMHD1*-deficient cells showed distinct mRNA expression patterns among more than 1200 genes (Figure 10). Pathway enrichment analysis revealed that the upregulated genes were associated significantly with the immune system, IFN signaling, and cytokine signaling pathways (Figure 11). Upstream regulator analysis predicted that various cytokines and

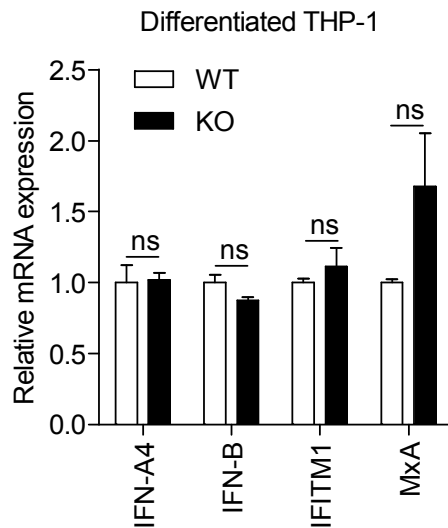


Figure 6. Differentiated THP-1 cells do not show a distinct IFN signature in *SAMHD1*-deficiency

qRT-PCR analysis of *IFN- α* , *IFN- β* , *IFITM1* and *MxA* in PMA-differentiated wild-type and *SAMHD1*-deficient THP-1 cells. Data were standardized to *β -actin*.

Data represent the mean \pm SEM of triplicate independent experiments (ns: not significant, two-tailed Student's t-test).

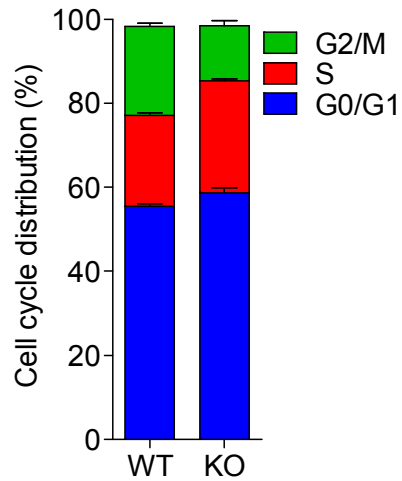


Figure 7. The effect of *SAMHD1*-deficiency on cell cycle distribution

Wild-type and *SAMHD1*-deficient cells were synchronized by serum starvation for 24 h, followed by the addition of serum for 24 h to induce cell cycle re-entry. Cells were harvested for propidium iodide staining and analyzed by FACS to determine the cell cycle distribution. The data represent the mean \pm SEM of triplicate independent experiments.

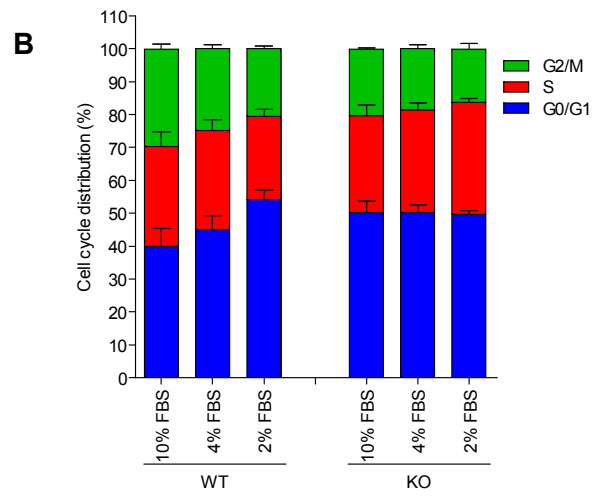
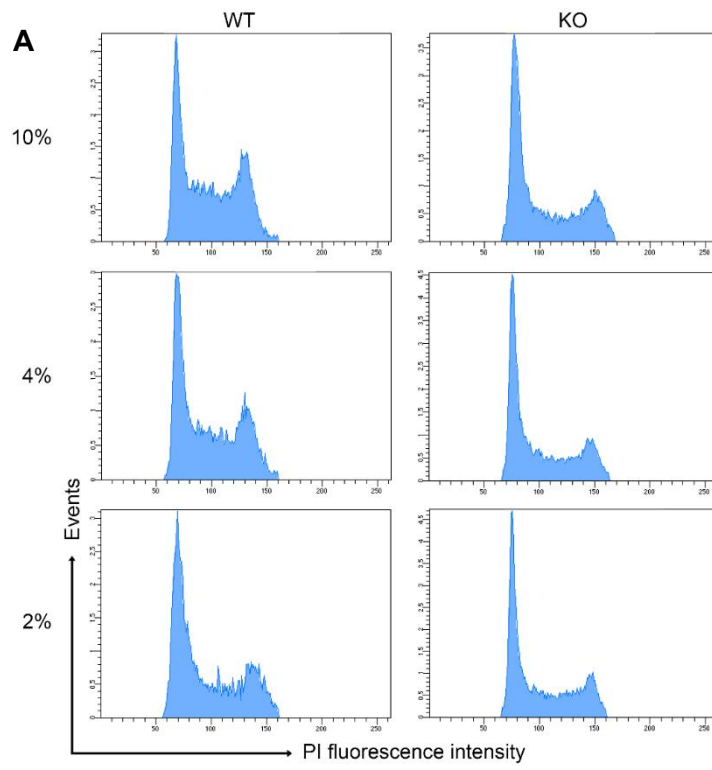


Figure 8. The effect of changes in serum concentration on the manipulation of cell cycle

(A, B) Wild-type and *SAMHD1*-deficient THP-1 cells were incubated in complete media containing 10 % FBS or reduced-serum media containing 4 % or 2 % FBS for 48 h, followed propidium iodide staining and FACS analysis to determine the cell cycle distribution. The data represent the mean \pm SEM of triplicate independent experiments.

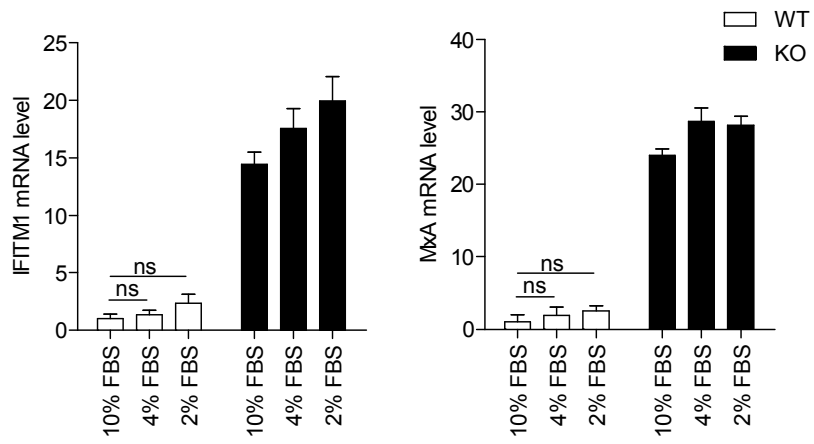


Figure 9. The manipulation of cell cycle is not responsible for the autoimmune phenotypes in *SAMHD1*-deficient cells

Wild-type and *SAMHD1*-deficient THP-1 cells were incubated in basal media containing 10 % FBS or reduced-serum media containing 4 % or 2 % FBS for 48 h, followed by qRT-PCR analysis of *IFITM1* and *MxA* mRNA levels. Data were standardized to *β-actin*. Data represent the mean ± SEM of triplicate independent experiments (ns: not significant, two-tailed Student's t-test).

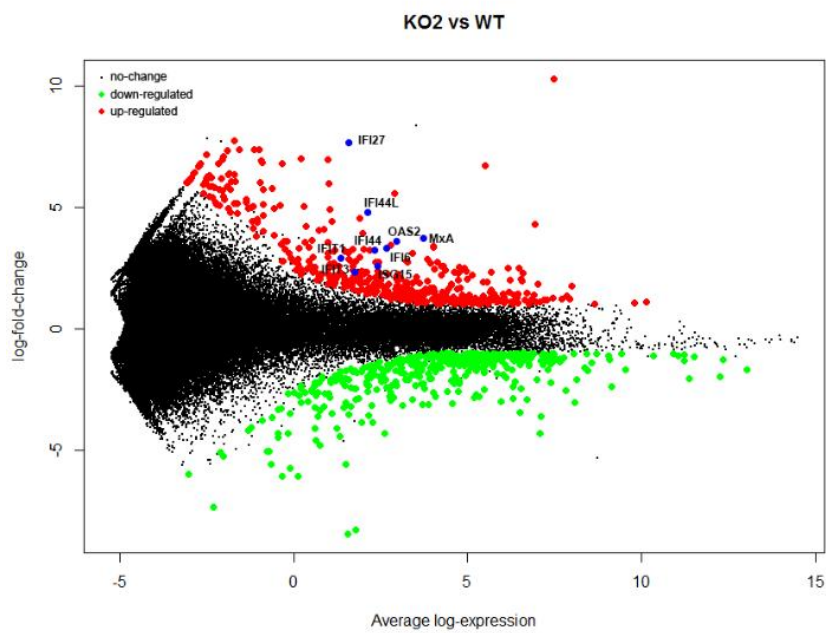
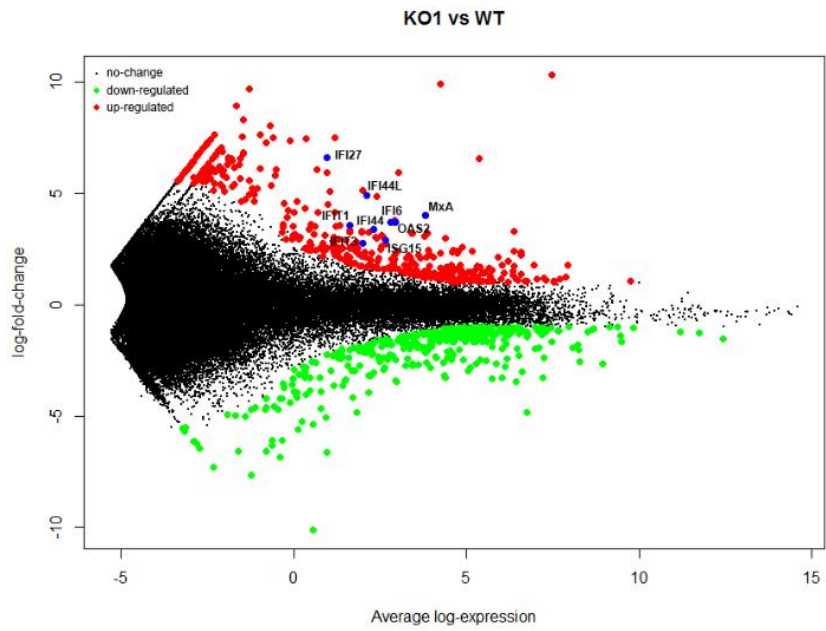


Figure 10. Identification of DEGs in *SAMHD1*-deficient THP-1 cells

RNA-seq MAplot of wild-type versus *SAMHD1* knockout cells as indicated. Three biological replicates were analyzed for both data sets. Average gene expression is plotted on the x-axis and log₂ fold-change is plotted on the y-axis; red dots: upregulated genes (log₂ FC ≥ 1 and adjusted p-values < 0.01), green dots: downregulated genes (log₂ FC ≤ -1 and adjusted p-values < 0.01), blue dots: ISGs.

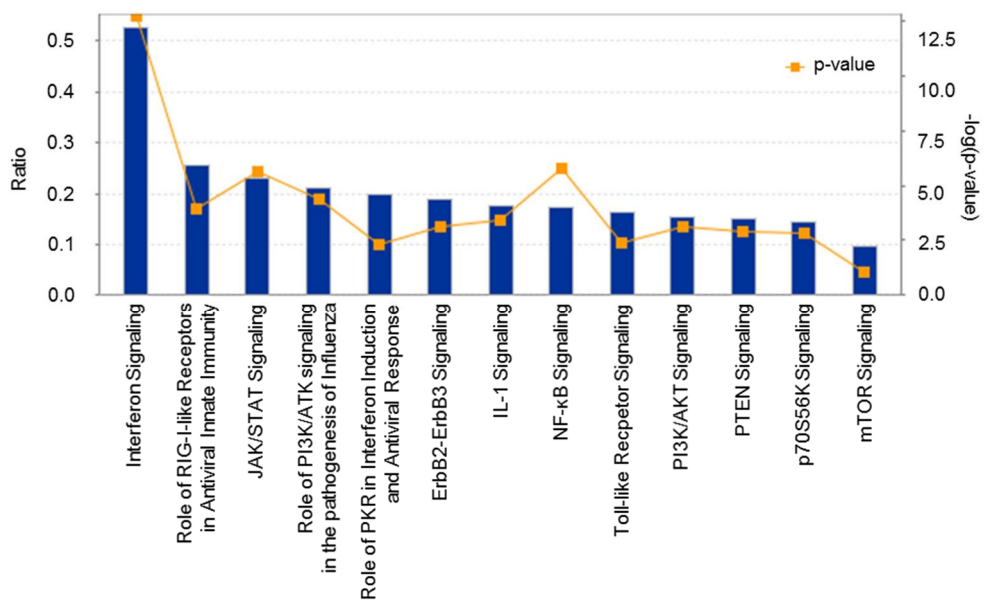


Figure 11. Classification of DEGs in *SAMHD1*-deficient THP-1 cells

Statistically significant signaling pathways for genes upregulated by over 2-fold in *SAMHD1* knockout samples were obtained by Ingenuity Pathway Analysis (IPA). Blue bars indicate the ratio of the total number of genes involved in the specific pathway versus input list genes, while the orange squares show $-\log$ (p-value).

transcription regulators related to the induction of type I IFN and ISGs would be activated (Figure 12). In particular, a broad range of ISGs were upregulated in *SAMHD1*-deficient cells (Figure 13), which closely resembled the IFN signature observed for patients with SLE and AGS (44). The expressions of several ISGs were validated by quantitative real-time reverse transcription polymerase chain reaction (qRT-PCR) (Figure 14). These results indicated that *SAMHD1*-deficient THP-1 cells show spontaneous autoimmune phenotypes.

2. RNA enriched in the absence of *SAMHD1* is a major source of the IFN- α response

I examined whether inappropriate accumulation of nucleic acids in *SAMHD1*-deficient cells activates IFN responses. I isolated both DNA and RNA from wild-type and *SAMHD1*-deficient cells and examined their abilities to stimulate the IFN response in PMA-differentiated THP-1 cells. Interestingly, only RNA derived from *SAMHD1*-deficient cells, but not that from wild-type cells, highly activated *IFN- α* expression. On the other hand, DNA isolated from wild-type and *SAMHD1*-deficient cells had comparable abilities to activate *IFN- α* expression (Figure 15A). RNA purified from *SAMHD1*-deficient cells had no discernible impact on the expression of *IFN- β* and *IFITM1* mRNA compared with RNA from wild-type cells (Figure 15B and 15C). Considering that the isolated RNAs are likely composed of various RNA species, the *IFN- β*

Upstream Regulator	Molecule Type	Predicted Activation State	p-value of overlap
IFNA2	cytokine	Activated	3.86E-25
IRF3	transcription regulator	Activated	4.48E-17
IRF7	transcription regulator	Activated	1.4E-15
IRF5	transcription regulator	Activated	1.38E-10
STAT1	transcription regulator	Activated	8.89E-10
IFNA1/IFNA13	cytokine	Activated	2.97E-09
IFNAR1	transmembrane receptor	Activated	1.45E-08
IFNB1	cytokine	Activated	2.56E-08

Figure 12. Bioinformatic prediction of the upstream regulators of DEGs in *SAMHD1*-deficient THP-1 cells

Bioinformatic analysis with IPA were performed to identify the upstream regulators of transcriptional regulation. Upstream regulator analysis in IPA sorted out type I IFN and IFN signature associated transcription regulators.

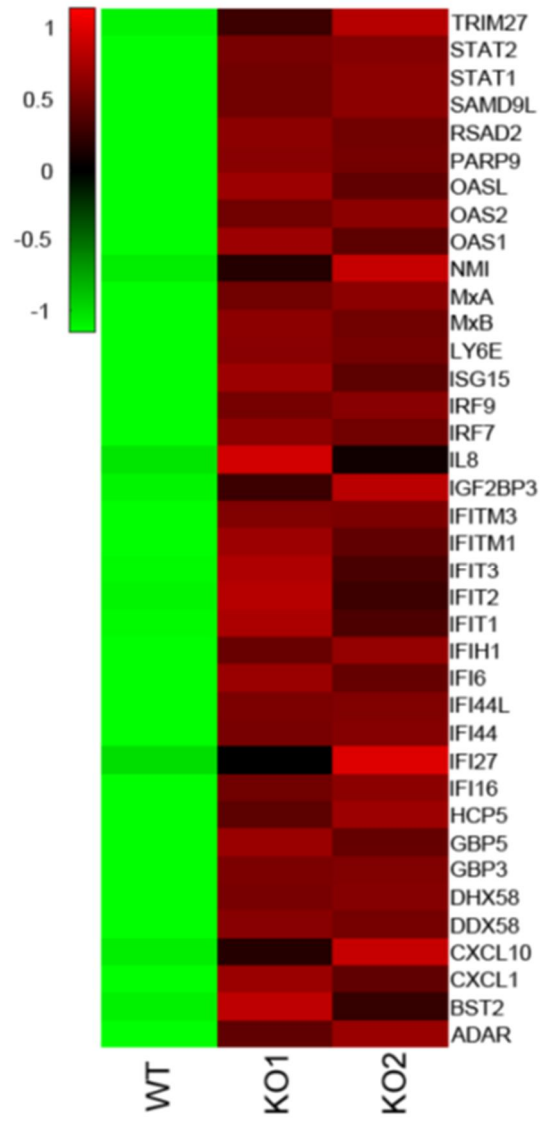


Figure 13. IFN signature in *SAMHD1*-deficient THP-1 cells

Heatmap of ISGs expressed in the indicated cells with the RNA-seq data. Gene expression levels (averaged reads per kilobase per million mapped reads (RPKM) values over 3 replicates) was standardized and clustered based on the dissimilarity values (1-Pearson correlation) between genes using the average linkage method as shown in the dendrogram.

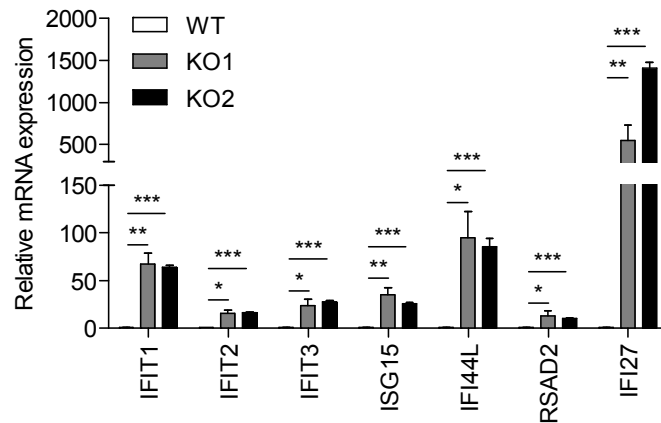


Figure 14. Verification of IFN signature in *SAMHD1*-deficient THP-1 cells

The mRNA levels of ISG genes in wild-type and *SAMHD1*-deficient THP-1 cells were determined by qRT-PCR. Data were normalized to the *GAPDH* level. Data represent the mean \pm SEM of triplicate independent experiments (* $p \leq 0.05$, ** $p \leq 0.01$, *** $p \leq 0.001$, two-tailed Student's t-test).

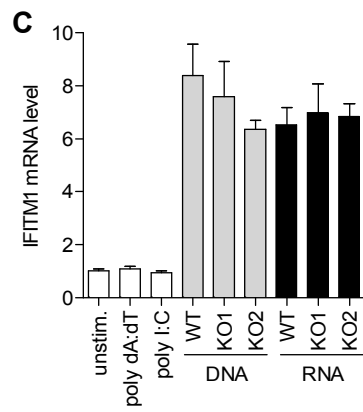
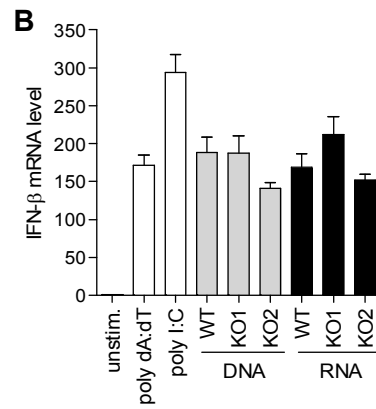
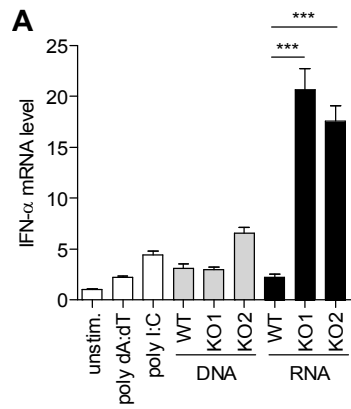


Figure 15. Accumulated RNAs in *SAMHD1*-deficient cells function as immune stimuli

(A-C) PMA-differentiated wild-type THP-1 cells were stimulated with poly dA:dT, poly I:C, an equal amount (5 µg/ml) of isolated total DNA and RNA from wild-type and *SAMHD1*-deficient cells, or left unstimulated. The mRNA levels of *IFN-α*, *IFN-β* and *IFITM1* were determined by qRT-PCR. Data were normalized to *β-actin* expression. Data represent the mean ± SEM of triplicate independent experiments (***) $p \leq 0.001$ two-tailed Student's t-test).

induction by RNA species that activate retinoic acid-inducible gene-I (RIG-I) or melanoma differentiation associated gene 5 (MDA5)-dependent pathways could mask the *IFN-β* induction by RNA substrates of SAMHD1. To investigate the detailed features of IFN-stimulatory RNA species, I isolated small (<200 nt) and large (>200 nt) RNAs in two separate fractions from each of the wild-type and *SAMHD1*-deficient THP-1 cell lines and then stimulated PMA-differentiated THP-1 cells with these RNAs. The large RNAs (>200 nt) from *SAMHD1*-deficient cells activated *IFN-α* mRNA expression significantly (Figure 16A) and showed similar effects on the induction of *IFN-β* or *IL-6* mRNA compared with the large RNAs (>200 nt) from wild-type cells (Figure 16B and 16C). Cell fractionation experiments also revealed that the cytoplasmic, but not the nuclear, RNA of *SAMHD1*-deficient cells induced *IFN-α* expression dominantly (Figure 17). My data suggested that the cytoplasmic RNA (>200 nt) accumulated in the absence of SAMHD1 triggers the IFN response. To investigate the discrepancy of type I IFN response in the absence of SAMHD1 between undifferentiated and differentiated THP-1 cells, I repeated the experiment for RNA stimulation with RNA isolated from differentiated wild-type and *SAMHD1*-deficient THP-1 cells. These RNAs did not show significant differences in activating type I IFN response (Figure 18), suggesting that the expression and accumulation of RNA substrates of SAMHD1 are differentially regulated after differentiation of monocytes (47, 48) and these differences

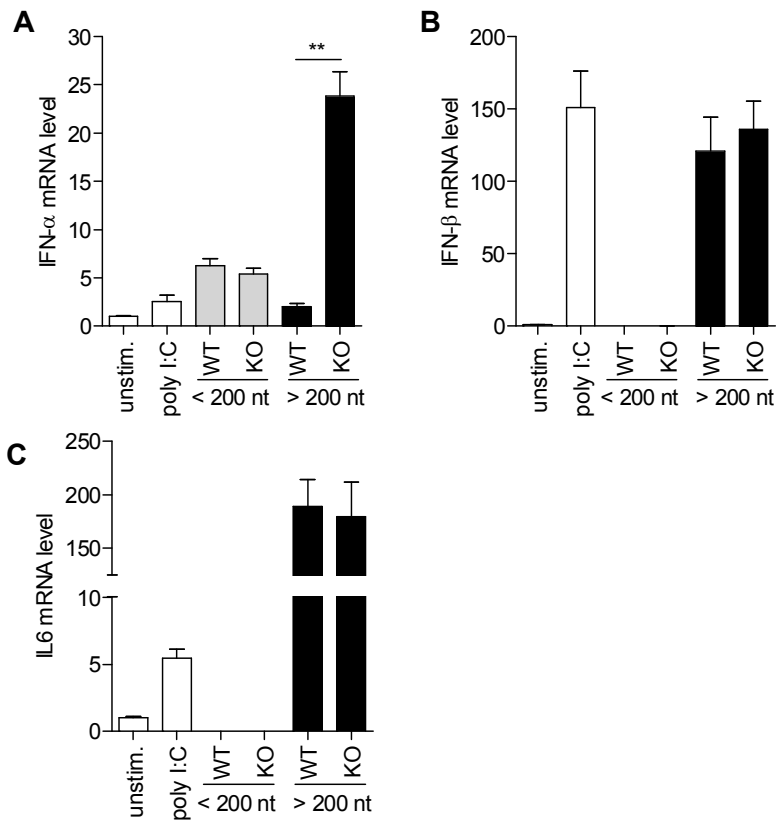


Figure 16. Large RNAs in *SAMHD1*-deficient cells function as immune stimuli

(A-C) Total RNA isolated from wild-type and *SAMHD1*-deficient cells were further size-fractionated and an equal amount of RNA from each fraction was used to stimulate PMA-differentiated wild-type THP-1 cells, followed by qRT-PCR analysis of *IFN- α* , *IFN- β* and *IL6* mRNA levels. Data were normalized to *β -actin* expression. These data represent the mean \pm SEM of triplicate independent experiments (** $p \leq 0.01$, two-tailed Student's t-test).

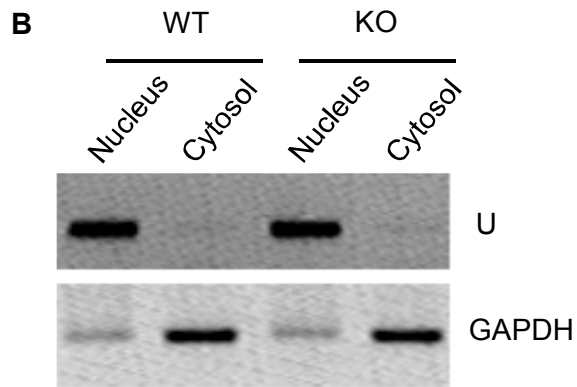
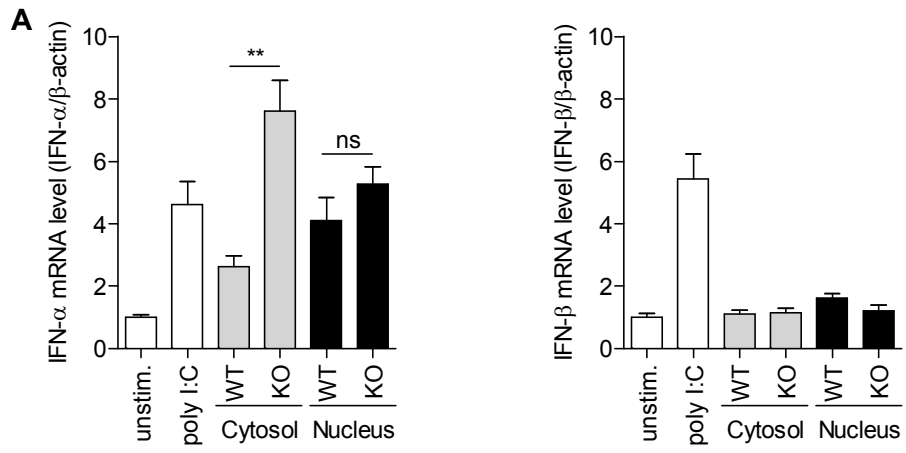


Figure 17. Cytoplasmic RNA from *SAMHD1*-deficient cells activates a type I IFN response

(A) qRT-PCR analysis of *IFN- α* and *IFN- β* expression in wild-type THP-1 cells stimulated with the nuclear or cytoplasmic RNA purified from wild-type and *SAMHD1*-deficient cells. Data represent the mean \pm SEM of triplicate independent experiments (** $p \leq 0.01$, ns: not significant, two-tailed Student's t-test). (B) RNA recovered from nuclear and cytoplasmic fractions was converted into cDNA. The cDNA was used for PCR amplification of *U6* and *GAPDH*. *U6* and *GAPDH* were used as markers for the quality of the fractionation.

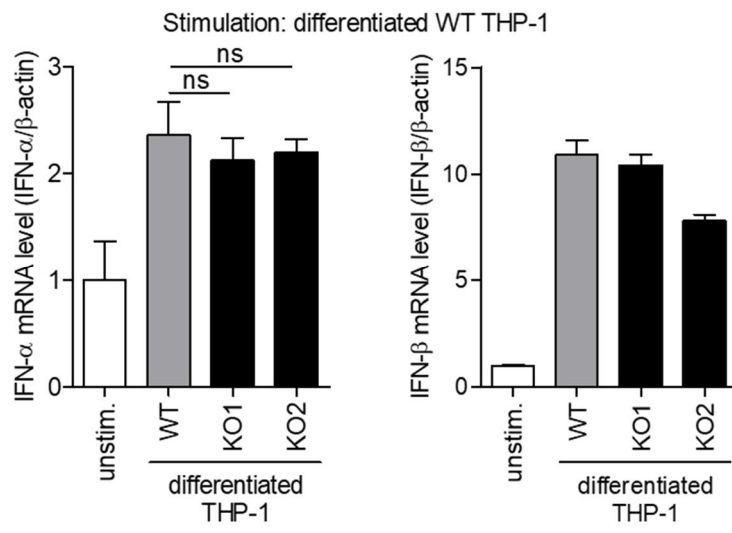


Figure 18. RNA from PMA-differentiated *SAMHD1*-deficient cells do not induce distinct *IFN- α* expression

PMA-differentiated wild-type THP-1 cells were stimulated with 5 μ g/ml of RNA isolated from PMA-differentiated wild-type and *SAMHD1*-deficient cells, or left unstimulated. The mRNA levels of *IFN- α* and *IFN- β* were determined by qRT-PCR. Data represent the mean \pm SEM of triplicate independent experiments (ns: not significant, two-tailed Student's t-test).

cause the cell type specificity of SAMHD1 related autoimmune response. Furthermore, I performed the RNA stimulation with RNA purified from undifferentiated wild-type and *SAMHD1*-deficient cells into undifferentiated wild-type or *SAMHD1*-deficient cells. Consistent with the data with differentiated THP-1 cells, RNA derived from *SAMHD1*-deficient cells distinctly activated *IFN- α* expression (Figure 19A and 19B). The activation of IFN response in undifferentiated cells was relatively mild compared to that of differentiated THP-1 cells. However, RNAs isolated from *SAMHD1*-deficient cells activated *IFN- α* expression about 3-fold higher than the RNAs isolated from wild-type cells in both undifferentiated wild-type and *SAMHD1*-deficient THP-1 cells. Thus, it seems that SAMHD1 could not efficiently degrade the transfected RNA, even though SAMHD1 degrades endogenous RNA species via its RNase activity.

SAMHD1 possesses both dNTPase and RNase activity, both of which are relevant to nucleic acid metabolism. I examined which of the two SAMHD1 functions is involved in the regulation of the type I IFN response. The RNase activity of SAMHD1 in undifferentiated THP-1 cells has not been characterized. Therefore, I first examined whether the SAMHD1 protein immunopurified from undifferentiated THP-1 cells possesses RNase activity. Immunopurified SAMHD1 protein was able to digest single-stranded RNA efficiently (Figure 20A). To exclude the possibility that contaminated RNA exonuclease during SAMHD1 purification might be responsible for the observed RNase activity, I

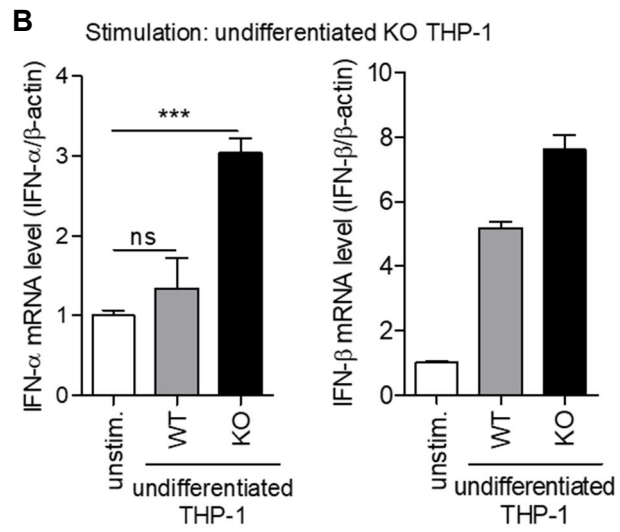
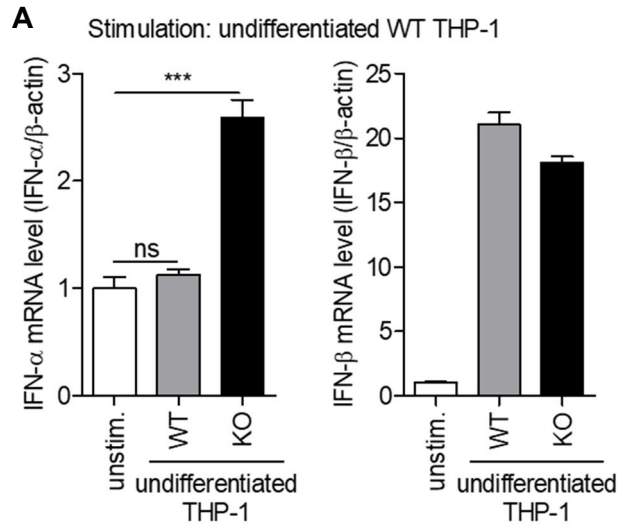


Figure 19. RNA from *SAMHD1*-deficient cells activates a type I IFN response

Undifferentiated wild-type (**A**) or *SAMHD1*-deficient THP-1 cells (**B**) were stimulated with 10 µg/ml of RNA isolated from undifferentiated wild-type and *SAMHD1*-deficient cells, or left unstimulated. The mRNA levels of *IFN-α* and *IFN-β* were determined by qRT-PCR. Data represent the mean ± SEM of triplicate independent experiments (***p* ≤ 0.001, ns: not significant, two-tailed Student's t-test).

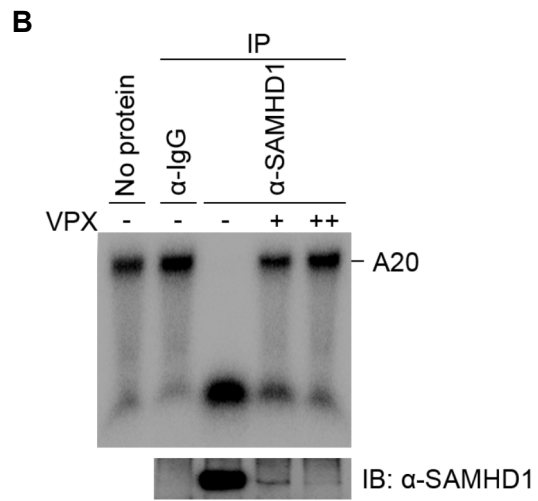
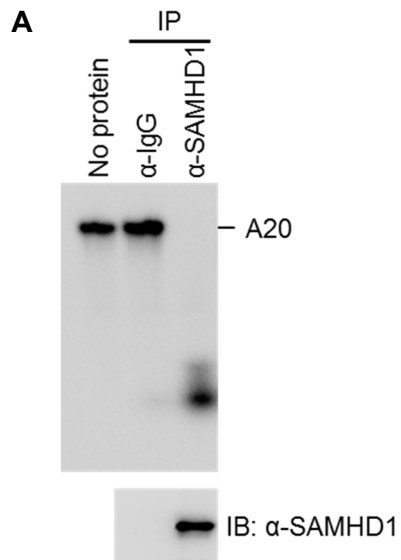


Figure 20. SAMHD1 protein immunopurified from undifferentiated THP-1 cells possesses RNase activity

(A, B) *In vitro* RNase activity assay for SAMHD1 immunopurified from undifferentiated THP-1 cells using A20 single-stranded RNA substrates. An isotype-matched control anti-IgG and anti-SAMHD1 antibodies were used for immunopurification. THP1 cells were infected with serial dilution of Vpx-loaded or control SIV VLPs **(B)**.

added Vpx-mediated SAMHD1 depleted controls (Figure 20B). Vpx-mediated degradation of SAMHD1 significantly reduced the enzymatic activity of immunopurified SAMHD1 protein, suggesting that SAMHD1 possesses RNase activity in undifferentiated THP-1 cells. Previously, my colleagues identified *SAMHD1* point mutations that caused loss of one or both functions; RNase⁻/dNTPase⁻ SAMHD1_{D207N}, RNase⁺/dNTPase⁻ SAMHD1_{D137N} and RNase⁻/dNTPase⁺ SAMHD1_{Q548A} (12). I reconstituted *SAMHD1*-deficient THP-1 cells with these SAMHD1 mutants using transient transfection and monitored the expression of *IFN-α* mRNA. SAMHD1_{D207N} and SAMHD1_{Q548A}, which have no RNase activity, did not repress the *IFN-α* induction. Notably, wild-type SAMHD1 and SAMHD1_{D137N} reduced the expression of *IFN-α* to the level observed in the mock control cells (Figure 21). These data supported the view that in *SAMHD1*-deficient cells, accumulation of incompletely digested RNAs leads to the activation of IFN response.

To gain the insight into the nature of cellular immune stimulatory RNA, I performed high-throughput sequencing of RNA isolated by crosslinking immunoprecipitation (HITS-CLIP) analysis with SAMHD1. Immunoprecipitates of SAMHD1 protein and SAMHD1-RNA complex were successfully detected by western blot and autoradiography (Figure 22A). A total of 5,500,000 peaks covering 38,000 genes including endogenous retroelements were called through SAMHD1 CLIP-seq. 60 % of these peaks were mapped to intronic

A

	Enzymatic activity	
	RNase	dNTPase
SAMHD1 _{WT}	+	+
SAMHD1 _{D137N}	+	-
SAMHD1 _{D207N}	-	-
SAMHD1 _{Q548A}	-	+

B

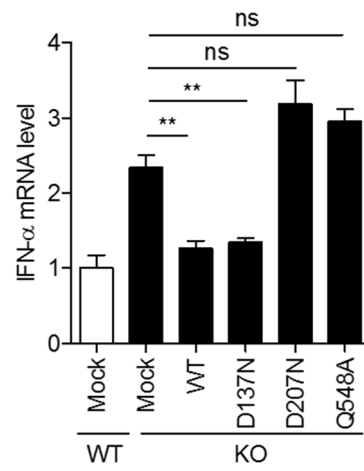
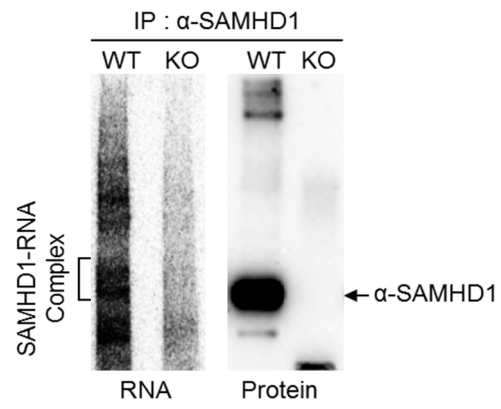


Figure 21. RNase activity of SAMHD1 is involved in the regulation of IFN response

(A) Enzymatic activity of SAMHD1 wild-type and mutants (B) qRT-PCR analysis of *IFN- α* in wild-type and *SAMHD1*-deficient cells reconstituted with indicated SAMHD1 wild-type and mutant constructs. Data were normalized to *β -actin* expression. In (B), this data represents the mean \pm SEM of triplicate independent experiments (** $p \leq 0.01$, ns: not significant, two-tailed Student's t-test).

A



B

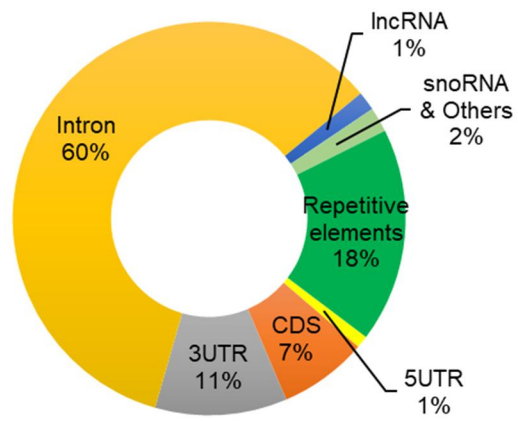


Figure 22. SAMHD1 CLIP-seq

(A) Autoradiography of SAMHD1-RNA complex and western blotting of SAMHD1 protein immunoprecipitated from SAMHD1 CLIP. (B) Pie chart showing the distribution of statistically significant peaks ($q < 0.001$) among the indicated RNA classes.

region, suggesting that SAMHD1 would function in nucleus during RNA processing or regulate RNA debris originated from intron in cytoplasm. 11 % of peaks were mapped to 3' UTR and only 8 % of peaks were mapped to 5' UTR and CDS region (Figure 22B). Notably, 18 % were repetitive elements that have been suggested as the source of endogenous immune stimulatory nucleic acid to account for AGS. My data showed that significant portion of the retroelement RNAs that are identified in SAMHD1 CLIP-seq were upregulated in *SAMHD1*-deficient cells. I, thus, speculate that these retroelement RNAs could be the substrates of SAMHD1 and function as immune stimulatory RNAs in *SAMHD1*-deficient cells.

3. ISG activation in *SAMHD1*-deficient cells is dependent on IRF3 & Type I IFN receptor

I sought to identify the RNA sensing pathway associated with ISG induction in *SAMHD1*-deficient cells. RIG-I-like receptors (RLRs), which include RIG-I and MDA5, and intracellular Toll-like receptors (TLRs) are well known cytosolic RNA sensors (49-52). I assumed that one of these RNA sensors might be linked to the IFN signature in *SAMHD1*-deficient cells. Therefore, I depleted each of these sensors or downstream molecules independently using short interfering RNA (siRNA) treatment (Figure 23). All of the known RNA sensors and intermediate signaling molecules, except Interferon Regulatory Factor 3

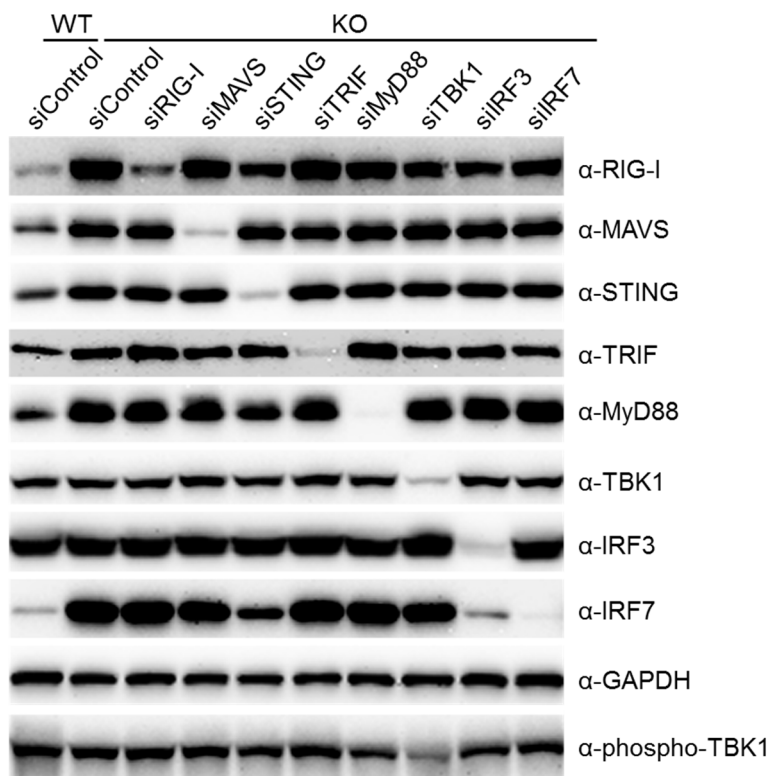


Figure 23. Depletion of nucleic acid sensors or downstream molecules using siRNA treatment

Wild-type and *SAMHD1*-deficient THP-1 cells were transfected with control siRNA or specific siRNA for the indicated genes for 72 h. Cell lysates were subjected to western blotting to analyze the protein levels. GAPDH was loaded as a control

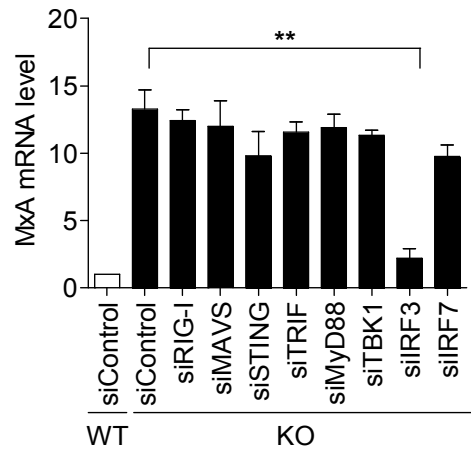
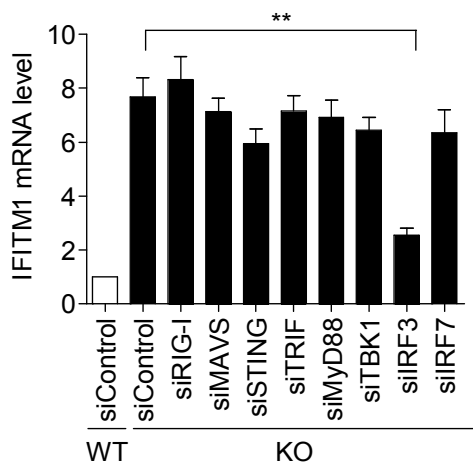


Figure 24. IRF3 is indispensable for ISGs induction in *SAMHD1*-deficiency

Wild-type and *SAMHD1*-deficient THP-1 cells were transfected with control siRNA or specific siRNA for the indicated genes for 72 h. The cellular mRNA was analyzed by qRT-PCR to determine the expression of *IFITM1* and *MxA* relative to *GAPDH*. These data represent the mean \pm SEM of triplicate independent experiments. (** $p \leq 0.01$, two-tailed Student's t-test).

(IRF3), were dispensable for the spontaneous IFN signature in *SAMHD1*-deficient cells (Figure 24). IRF3 depletion in *SAMHD1*-deficient cells abrogated the expression of *IFITM1* and *MxA* to near the levels of wild-type THP-1 cells. Activation of almost known RNA sensing pathways requires the phosphorylation of TBK1, which acts upstream of IRF3. Notably, phosphorylated TBK1 levels were similar between wild-type and *SAMHD1*-deficient cells (Figure 23), suggesting that a novel RNA sensing pathway is responsible for the IFN response observed in *SAMHD1*-deficient cells.

To investigate whether the proteins secreted from *SAMHD1*-deficient cells boost ISG induction, I harvested the conditioned media from wild-type and *SAMHD1*-deficient THP-1 cells. The conditioned media from both wild-type and *SAMHD1*-deficient cells did not exhibit any significant differential ability to stimulate IFN- α expression. However, wild-type THP-1 cells treated with the conditioned media from *SAMHD1*-deficient cells displayed significantly elevated ISG levels in a time-dependent manner (Figure 25). Both type I (IFN- α and IFN- β) and type III (IFN- λ) IFNs can lead to the similar spectrum of ISG induction. To identify the discrete contribution of type I and type III IFNs to ISG induction, *SAMHD1*-deficient cells were treated with neutralizing antibodies directed against the type I and III IFN receptor subunits, IFNAR1 and IL10R β , respectively. Neither the anti-IFNAR1 nor anti-IL10R β antibodies reduced the

expression of type I IFN in *SAMHD1*-deficient cells. However, the expressions

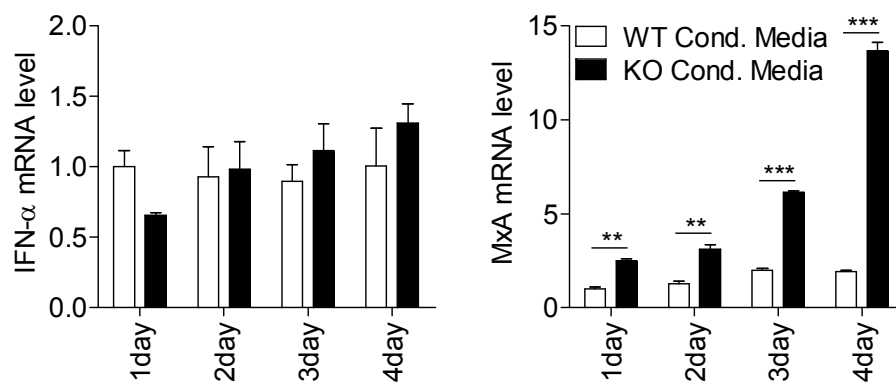


Figure 25. Secreted proteins from *SAMHD1*-deficient cells elevate ISG levels in a time-dependent manner

qRT-PCR analysis of *IFN- α* and *MxA* in THP-1 cells incubated with conditioned media (Cond. Media.) from wild-type or *SAMHD1*-deficient cells for the indicated days. Data were standardized to *GAPDH*. Data represent the mean \pm SEM of triplicate independent experiments. (** $p \leq 0.01$, *** $p \leq 0.001$, two-tailed Student's t-test).

of ISGs (*IFITM1* and *MxA*) were reduced to basal levels in cells treated with anti-IFNAR1, but not in those treated with the anti-IL10R β antibody. Co-treatment with both IFNAR1 and IL10R β antibodies did not show synergistic inhibitory effects on ISGs induction (Figure 26). Thus, I concluded that type I IFN is responsible for the IFN signature observed in *SAMHD1*-deficient cells. Type I IFN receptors associate with Janus activated kinases (JAKs), and activation of the Janus kinase/signal transducers and activators of transcription (JAK/STAT) pathway is indispensable for ISGs induction (53). JAK inhibitor treatment diminished ISG induction thoroughly (Figure 27). Taken together, these findings indicated that the type I IFN secreted by the IRF3-dependent novel RNA sensing pathway activates ISG induction, which could be responsible for AGS pathogenesis.

4. The PI3K/AKT signaling pathway is involved in linking *SAMHD1*-deficiency to the IFN response

Type I IFN can activate multiple signaling pathways, including the JAK/STAT pathway, the p38 and extracellular signal-regulated kinase (ERK) pathways, and the phosphoinositide 3-kinase (PI3K)/AKT pathway (54). Pathway enrichment analysis of genes upregulated in *SAMHD1*-deficient cells showed a significant enrichment of genes related to the PI3K/AKT pathway (Figure 11).

Indeed, STAT1 and AKT were highly activated in *SAMHD1*-deficient cells, as

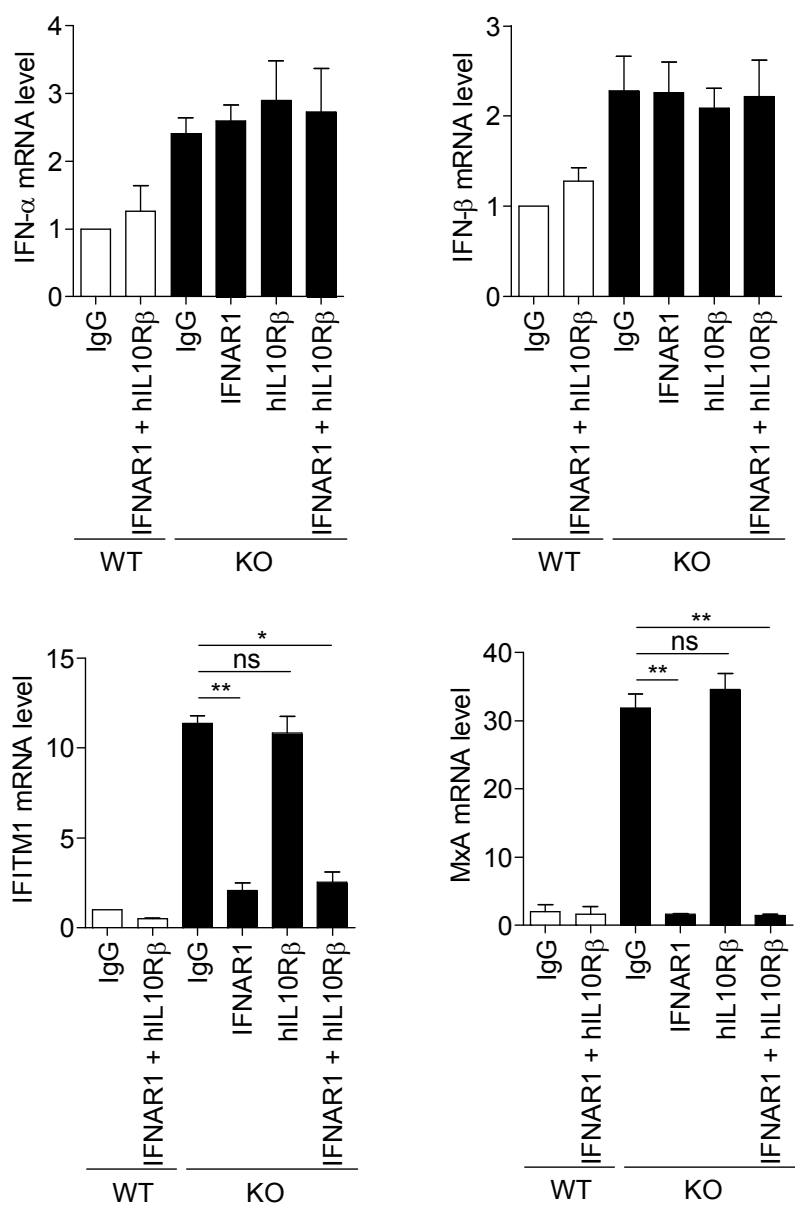


Figure 26. ISGs induction in *SAMHD1*-deficiency occurs through type I IFN receptor signaling pathway

qRT-PCR analysis of *IFN- α* , *IFN- β* , *IFITM1* and *MxA* in wild-type and *SAMHD1*-deficient THP-1 cells treated with control IgG or neutralizing antibodies against type I and III IFN receptor subunits as indicated. Results were standardized to *β -actin* levels. These data represent the mean \pm SEM of triplicate independent experiments. (* $p \leq 0.05$, ** $p \leq 0.01$, ns: not significant, two-tailed Student's t-test).

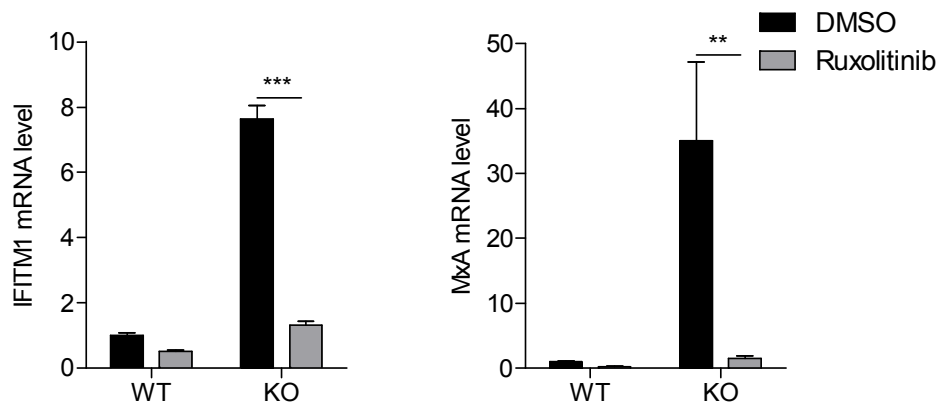


Figure 27. JAK inhibitor treatment diminishes ISG induction

The measurement of *IFITM1* and *MxA* mRNA expressions in *SAMHD1*-deficient cells by qRT-PCR after treating *SAMHD1*-deficient cells with control dimethylsulfoxide (DMSO) or 2 μ M Ruxolitinib for 24 h. Data were standardized to *GAPDH*. Data represent the mean \pm SEM of triplicate independent experiments. (** $p \leq 0.01$, *** $p \leq 0.001$, two-tailed Student's t-test).

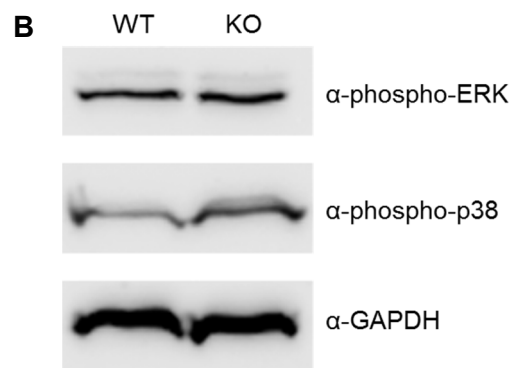
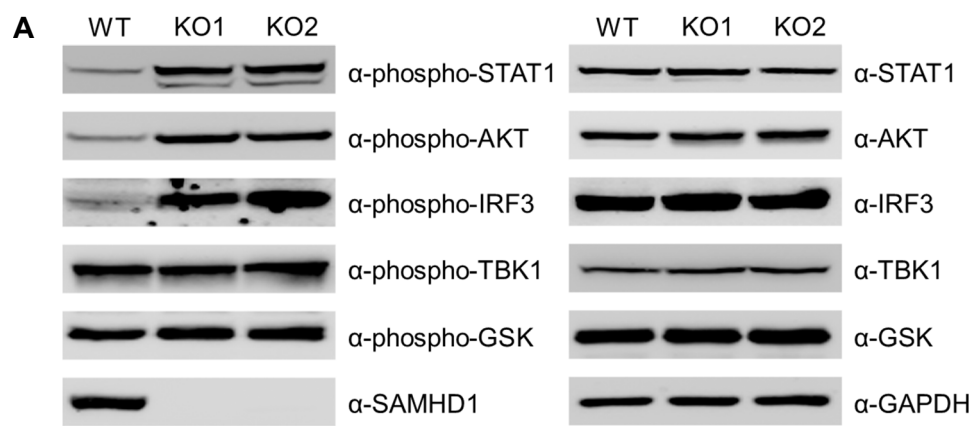


Figure 28. AKT is highly activated in *SAMHD1*-deficient cells

(**A, B**) Western blotting analysis of cell extracts from wild-type and two independent *SAMHD1*-deficient cell lines using the indicated antibodies. GAPDH served as a loading control.

assessed by the phosphorylation levels of these molecules (Figure 28A). IRF3 was also activated in *SAMHD1*-deficient cells, which agreed with the observation that depletion of IRF3 abrogates ISG induction (Figure 24). However, p38 and ERK pathways were not activated in *SAMHD1*-deficient cells (Figure 28B). To ascertain the role of the PI3K/AKT pathway in the *SAMHD1*-related IFN response, I treated *SAMHD1*-deficient cells with wortmannin, a PI3K inhibitor. Wortmannin inhibited not only the induction of type I IFN and ISGs but also the activation of AKT and STAT1 (Figure 29 and Figure 30). Treatment of *SAMHD1*-deficient cells with the pan-AKT inhibitor MK2206 or the AKT1 inhibitor A674563 reduced the IFN signature. By contrast, inhibition of the PI3K upstream tyrosine kinase using Lapatinib and inhibition of mTOR, a downstream effector of AKT, using rapamycin did not affect the IFN signature (Figure 31). Consistent with these data, the activation of STAT1 is also abrogated by AKT inhibitors treatment (Figure 32). To confirm the data obtained from the pharmacological studies, I generated the *SAMHD1/AKT1* double knockout cells via the CRISPR/ CRISPR associated protein9 (Cas9) system. Phosphorylation of STAT1 and IRF3 induced by *SAMHD1* knockout was markedly diminished upon *SAMHD1/AKT1* double knockout (Figure 33). Type I IFN production and ISGs induction also significantly decreased in *SAMHD1/AKT1* double knockout cells (Figure 34). Glycogen synthase kinase 3- β (GSK3- β) regulates TLR4 mediated IFN- β production negatively (55). The

phosphorylation levels of GSK3- β were similar in the wild-type and *SAMHD1*-

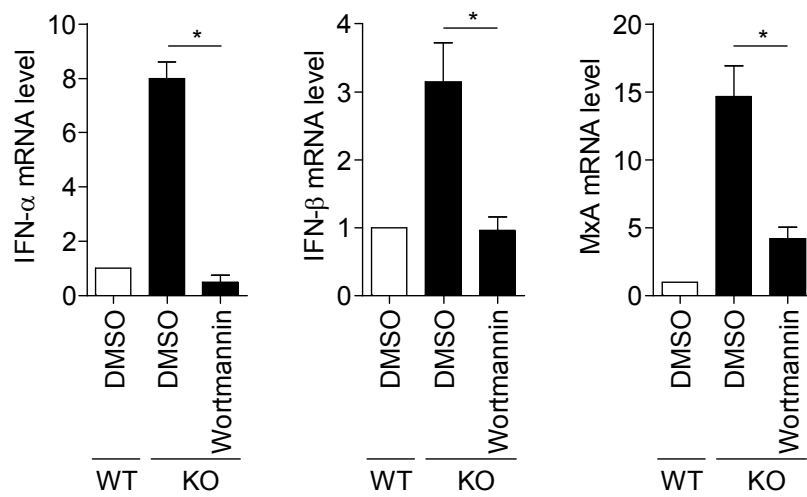


Figure 29. PI3K inhibitor blocks the induction of type I IFN and ISGs

qRT-PCR analysis of *IFN- α* , *IFN- β* and *MxA* levels in wild-type and *SAMHD1*-deficient THP-1 cells treated with control DMSO or 1 μ M Wortmannin for 24 h. Data were normalized to *GAPDH* levels. Data represent the mean \pm SEM of triplicate independent experiments (* $p \leq 0.05$, two-tailed Student's t-test).

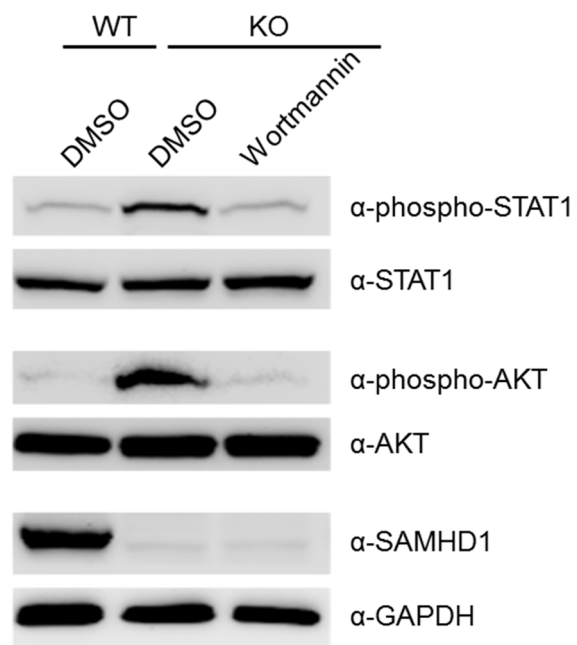


Figure 30. PI3K inhibitor suppresses the activation of STAT1 and AKT

Wild-type and *SAMHD1*-deficient THP-1 cells were treated with control DMSO or 1 μ M Wortmannin for 24 h. Cell lysates were analyzed for the western blotting analysis to determine the phosphorylation status of STAT1 and AKT. GAPDH serves as a loading control.

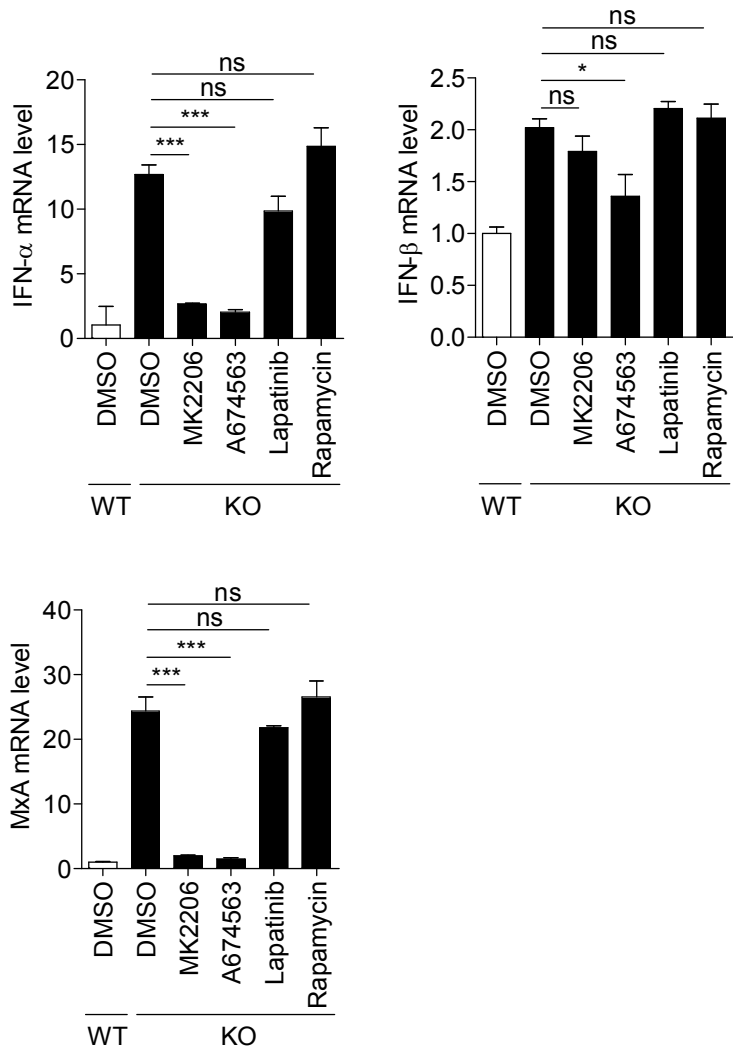


Figure 31. AKT inhibitor diminishes the induction of type I IFN and ISGs

Wild-type and *SAMHD1*-deficient THP-1 cells were treated with control DMSO, 1 μ M MK2206, 1 μ M A674563, 0.1 μ M Lapatinib or 50 nM Rapamycin for 24 h. Cells were analyzed for the mRNA levels of *IFN- α* , *IFN- β* and *MxA* relative to *GAPDH* by qRT-PCR. Data represent the mean \pm SEM of triplicate independent experiments (* $p \leq 0.05$, *** $p \leq 0.001$, ns: not significant, two-tailed Student's t-test).

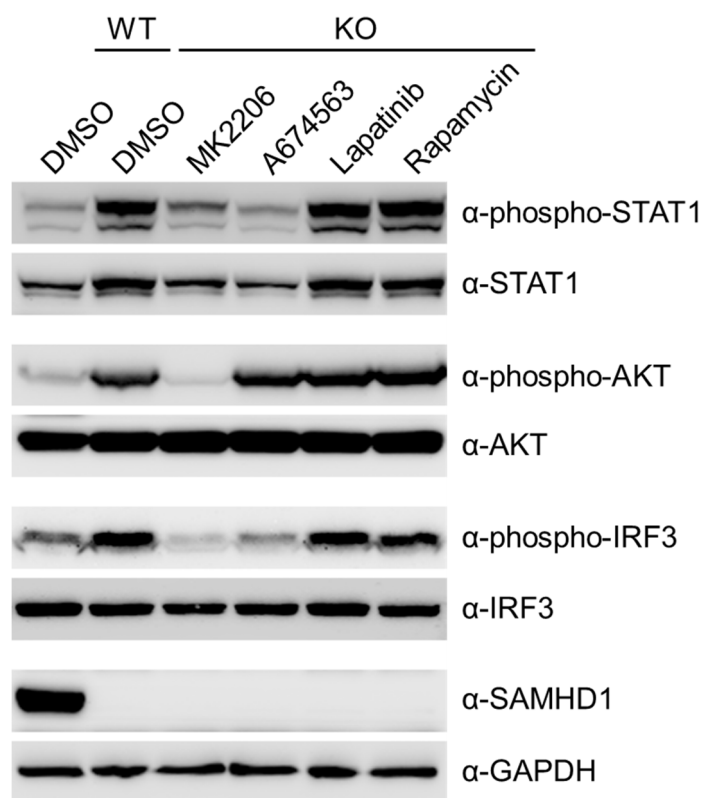


Figure 32. AKT inhibitor abolishes the activation of STAT1 and AKT

Wild-type and *SAMHD1*-deficient THP-1 cells were treated with control DMSO or 1 μ M Wortmannin for 24 h. Cell lysates were analyzed for the western blotting analysis to determine the phosphorylation status of STAT1 and AKT. GAPDH serves as a loading control.

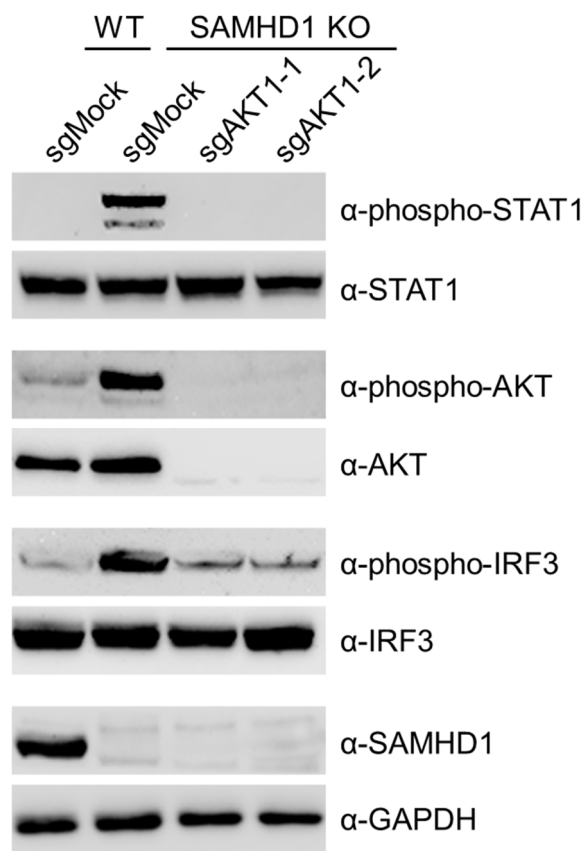


Figure 33. *AKT* knockout abrogates the activation of IRF3 and STAT1 in *SAMHD1*-deficient cells

The phosphorylation status of STAT1 and IRF3 in wild-type, *SAMHD1* knockout and *SAMHD1/AKT* double-knockout THP-1 cells was determined by western blotting analysis. GAPDH served as a loading control.

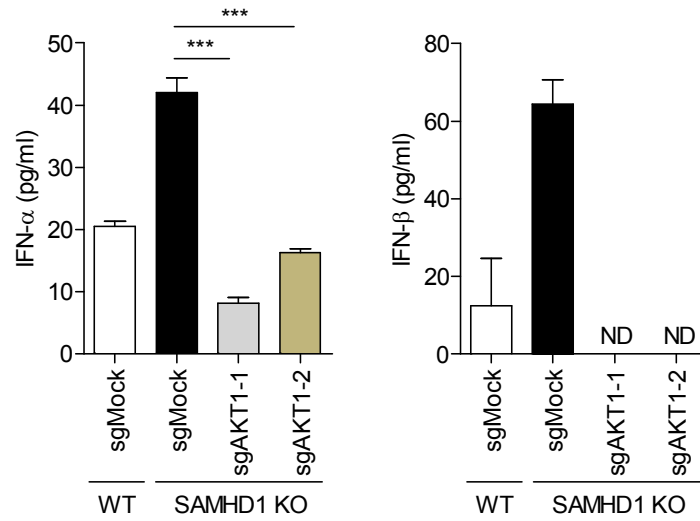
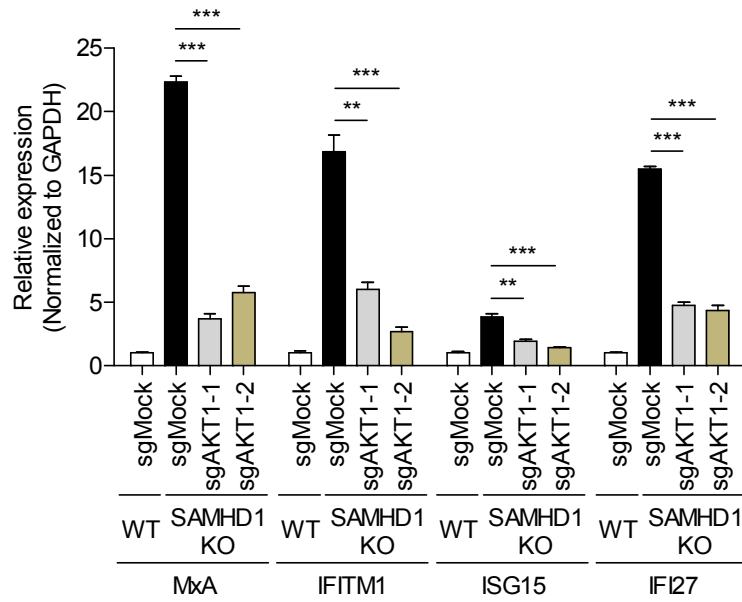
A**B**

Figure 34. AKT knockout abrogates SAMHD1-associated AGS phenotypes

(A, B) Determination of type I IFN and ISGs production in *SAMHD1/AKT1* double knockout THP-1 cells compared with wild-type and *SAMHD1* single knockout cells. Using independent sgRNAs (sgAKT1-1 and sgAKT1-2) targeting *AKT1*, two independent *SAMHD1/AKT* double knockout clones with a *SAMHD1*-null background were established and used for the experiments. IFN- α in cell extracts and IFN- β in supernatants were measured using an ELISA. ND, not detectable **(A)**. The expression of ISGs (*MxA*, *IFITM1*, *ISG15* and *IFI27*) in the same samples as in A was measured by qRT-PCR, normalized to *GAPDH* expression **(B)**. Data represent the mean \pm SEM of triplicate independent experiments (** $p \leq 0.01$, *** $p \leq 0.001$, two-tailed Student's t-test).

deficient cells (Figure 28A). Therefore, the SAMHD1-related type I IFN response is likely independent of the GSK3- β pathway. The PI3K/AKT pathway can be also activated by type I IFN. Thus, I attempted to clarify the cause-effect relationship between type I IFN production and activation of the PI3K/AKT pathway. First, I investigated whether treatment of AKT inhibitor abolishes the activation of IRF3. As reported, MK2206 inhibited AKT1 phosphorylation, while A674563, which blocks the phosphorylation of AKT downstream targets, does not. Both AKT inhibitors abrogate IRF3 phosphorylation (Figure 32). Neutralizing antibodies against the type I IFN receptor inhibited STAT1 phosphorylation, but not that of AKT or IRF3 (Figure 35). siRNA-mediated depletion of IRF3 diminished STAT1 phosphorylation, but not that of AKT (Figure 36), suggesting that the PI3K/AKT pathway functions upstream of IRF3 activation in the type I IFN-producing pathway. Taken together, these results showed that IFN production in *SAMHD1*-deficient cells occurs through the PI3K/AKT/IRF3 signaling axis.

The phosphorylation of AKT induced by *SAMHD1* knockout was antagonized by ectopic expression of wild-type SAMHD1 or RNase⁺/dNTPase⁻ SAMHD1_{D137N}. Expression of the RNase-defective mutants, SAMHD1_{D207N} and SAMHD1_{Q548A}, had little effect on AKT phosphorylation (Figure 37), which was consistent with the observation that the RNase activity of SAMHD1 is critical to suppress the spontaneous IFN response in *SAMHD1*-deficient cells (Figure 21).

To explore the physiological relevance of my findings, I analyzed the role

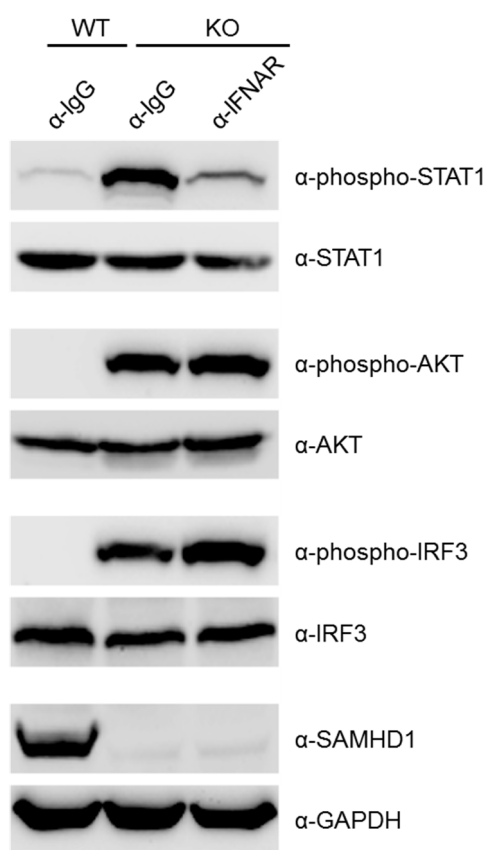


Figure 35. The PI3K/AKT functions upstream of type I IFN receptor signaling pathway

Western blotting analysis of cell extracts from wild-type and *SAMHD1*-deficient cells treated with control IgG or a neutralizing antibody against a type I IFN receptor subunit for 48 h. GAPDH served as a loading control.

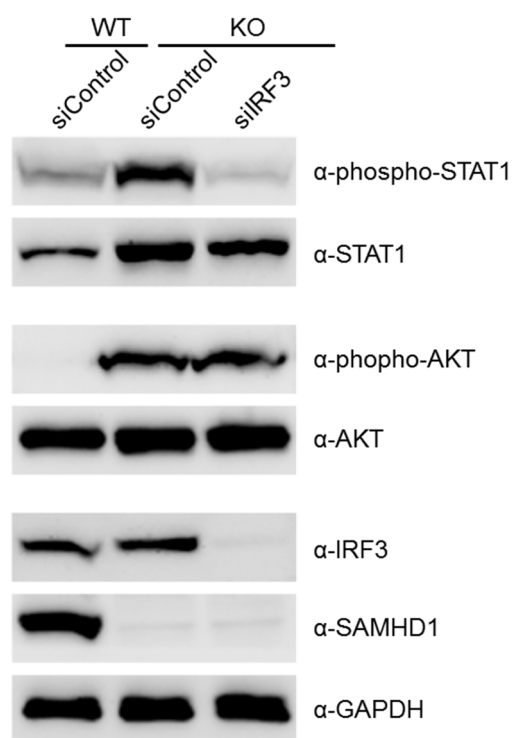


Figure 36. The PI3K/AKT functions upstream of IRF3 to activate type I IFN response

Western blotting analysis of cell extracts from wild-type and *SAMHD1*-deficient cells transfected with control non-specific siRNA or a specific siRNA for IRF3. GAPDH served as a loading control.

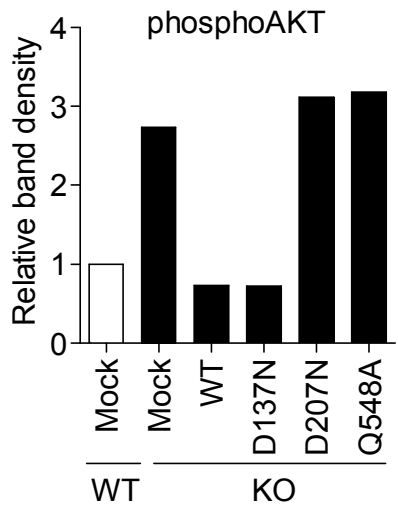
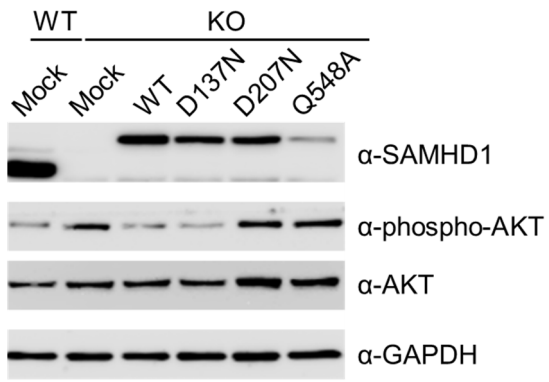


Figure 37. RNase activity of SAMHD1 is responsible for the activation of AKT

Determination of the phosphorylation status of AKT after reconstitution of *SAMHD1*-deficient cells with wild-type and *SAMHD1* mutants by western blotting analysis. Graph shown below indicates ratio of phosphoAKT to wild-type control.

for SAMHD1 in regulating an IFN response using human peripheral blood mononuclear cells (PBMCs). In human PBMCs, siRNA-mediated SAMHD1 silencing elicited the activation of STAT1 and AKT, but had no effect on TBK1 activation (Figure 38), recapitulating the phenotypes seen in *SAMHD1*-deficient THP-1 cells. By comparison, knockout of *SAMHD1* in HEK293T and HeLa cells did not result in activation of STAT1 and AKT or the induction of ISGs (Figure 39 and Figure 40), which suggested that the type I interferonopathy associated with *SAMHD1*-deficiency is cell type-specific.

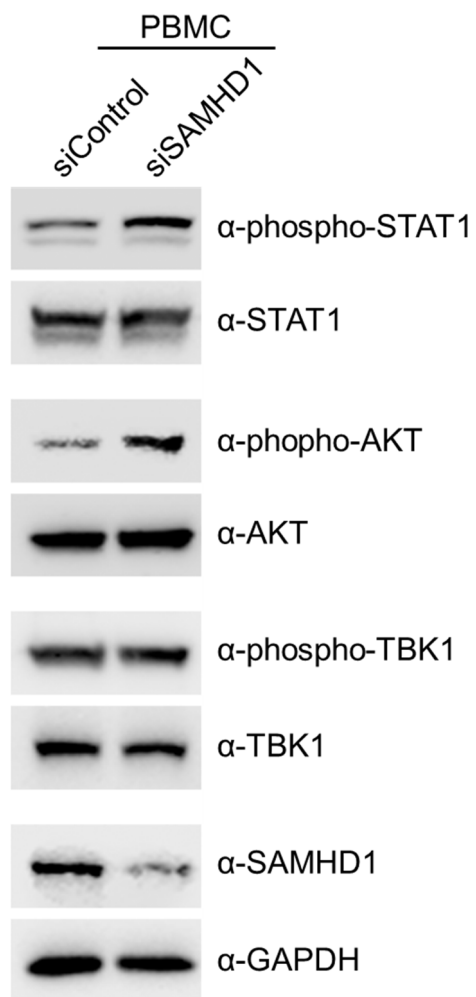


Figure 38. siRNA-mediated SAMHD1 silencing in human PBMCs recapitulates the phenotypes seen in SAMHD1-deficient THP-1 cells

Isolated PBMCs from four donors were transfected with SAMHD1-specific siRNA or control non-specific siRNA for two cycles to enhance the knockdown efficiency. After 48 h of incubation, PBMCs were analyzed by western blotting to monitor the activation of STAT1 and AKT. Data are representative of four independent experiments with similar results. GAPDH served as a loading control.

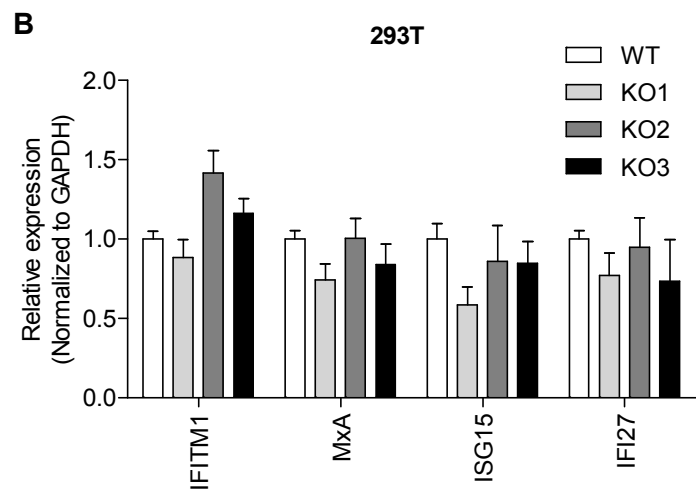
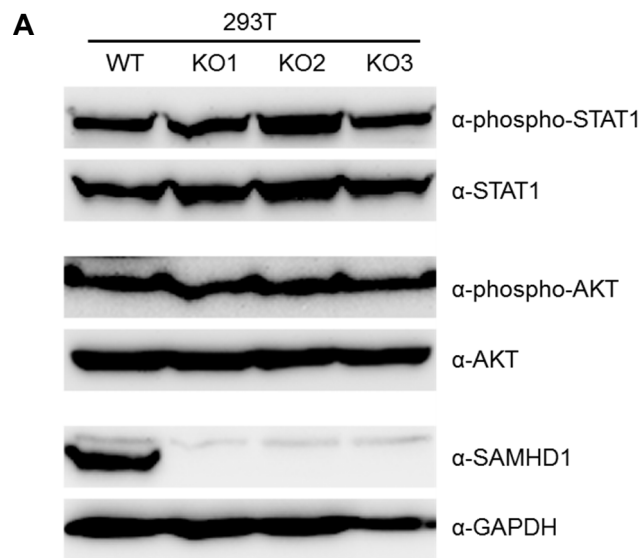


Figure 39. *SAMHD1*-deficient 293T cells do not display AGS phenotypes

(**A, B**) *SAMHD1*-deficient cell lines were constructed in 293T cells using the CRISPR/Cas9 system. Western blotting analysis of cell extracts from wild-type and *SAMHD1*-deficient 293T cells (**A**). Cell lysates were analyzed for the phosphorylation status of STAT1 and AKT with the indicated antibodies. GAPDH was loaded as a control. The expression of ISGs (*MxA*, *IFITM1*, *ISG15* and *IFI27*) in the same samples were measured by qRT-PCR, normalized to *GAPDH* expression (**B**).

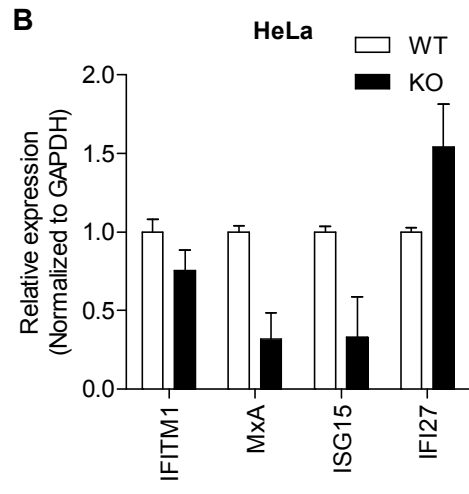
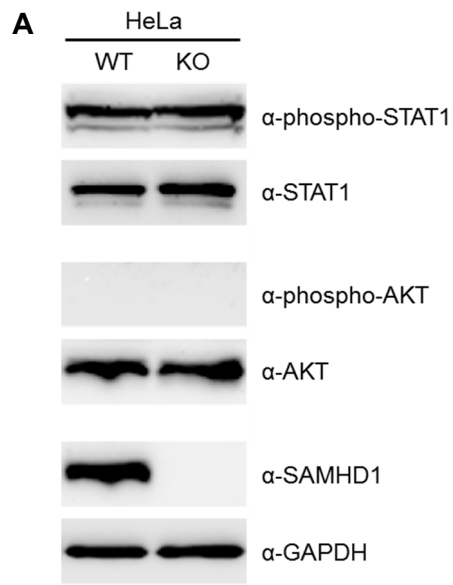


Figure 40. *SAMHD1*-deficient HeLa cells do not display AGS phenotypes

(**A, B**) *SAMHD1*-deficient cell lines were constructed in HeLa cells using the CRISPR/Cas9 system. Western blotting analysis of cell extracts from wild-type and *SAMHD1*-deficient HeLa cells (**A**). Cell lysates were analyzed for the phosphorylation status of STAT1 and AKT with the indicated antibodies. GAPDH was loaded as a control. The expression of ISGs (*MxA*, *IFITM1*, *ISG15* and *IFI27*) in the same samples were measured by qRT-PCR, normalized to *GAPDH* expression (**B**).

DISCUSSION

SAMHD1 had been identified as HIV-1 restriction factor in the last decade and it was initially reported to inhibit HIV-1 replication through its dNTPase activity (24, 25). Later my colleagues reported that SAMHD1 restricts HIV-1 and retroviruses through its RNase activity (12, 56). However, several studies reported that they have not observed the RNase activity of SAMHD1, even though SAMHD1 could bind nucleic acids such as ssRNA (30, 57). To clarify this discrepancy, my colleagues recently showed that SAMHD1 is a phospholytic exoribonuclease with A or U base preference (13). Nevertheless, the existence of RNase activity of SAMHD1 is still being debated.

The current study identified the signaling mechanism driving the chronic upregulation of type I IFN in AGS related to *SAMHD1*-deficiency. My findings showed that the RNA species larger than 200 nucleotides that accumulated in *SAMHD1*-deficient cells trigger a type I IFN response. More specifically, I observed that cytosolic RNA species larger than 200 nucleotides are responsible for the type I IFN induction. This type I IFN response does not involve any of the known signaling pathways converging on the activation of TBK1. Instead, the type I IFN response occurs via a novel PI3K/AKT/IRF3 signaling pathway. Consequently, ISGs are induced in bystander cells via a type I IFN receptor- and JAK/STAT-dependent manner (Figure 41).

In contrast to AGS patients with mutations in *SAMHD1* (32), *Samhd1*-deficient mice did not exhibit any distinct clinical phenotypes (42, 43). The discrepancy between the mouse and human systems in terms of SAMHD1-

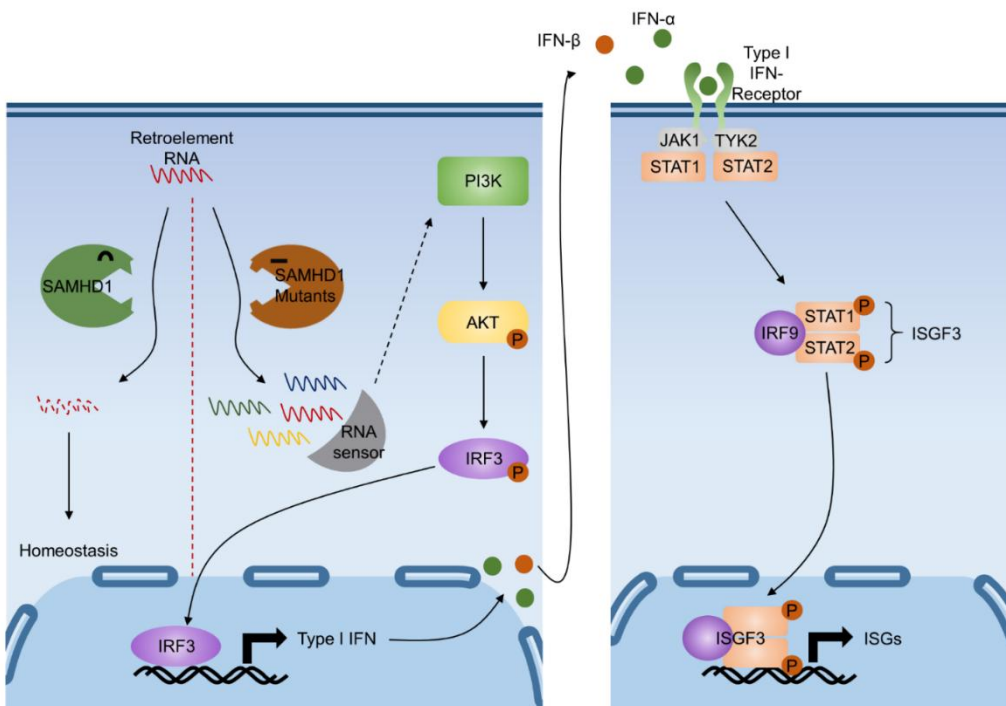


Figure 41. A working model for SAMHD1-related interferonopathy in AGS

Based on the current study, we propose a working model for linking *SAMHD1*-deficiency to a type I IFN response. In the absence of functional *SAMHD1*, inappropriately metabolized RNAs accumulate in cells. An unknown RNA sensor recognizes the accumulated RNAs and triggers the downstream activation of the PI3K/AKT signaling pathway, resulting in the expression of type I IFN through IRF3 activation. Finally, binding of type I IFN to the type I IFN receptors of bystander cells activates the JAK/STAT signaling pathway, leading to the induction of ISGs.

related IFN responses might arise from differences in the putative nucleic acid substrates of SAMHD1. There are striking differences between the mouse and human ERVs/LTR elements in terms of their activities, tissue specific expression and temporal regulation during development (58, 59). Given the propensity of these ERVs/LTR elements to affect gene expression, the differences of the repertoire of ERVs/LTR elements could account for the differential susceptibilities of humans and mice to SAMHD1-regulated IFN responses. Another possibility is that an unknown RNA sensor or other components involved in the constitutive IFN-induced signaling pathway could be missing in mice. Recently, a study reported that a cGAS/STING-dependent IFN response is triggered in *Samhd1*-deficient mice, although that study did not address which substrates are involved in the IFN response (60). Mice contain “active” LTR elements and significant ERV activity (58). By contrast, “active” ERVs/LTR elements in humans, while present in comparable numbers, have not been reported (61). Thus, the reverse transcribed DNAs originating from the mouse ERVs/LTR elements might be a predominant source of the cGAS/STING-mediated IFN response. Furthermore, these disparities could cause the discrepancy of the source of IFN response between humans and mice, leading to the absence of systemic autoimmune phenotypes in *Samhd1*-deficient mice compared with SAMHD1-related AGS patients.

Notably, SAMHD1 specifically targets retroviral RNA for degradation (12, 56). Even though SAMHD1-CLIP failed to identify dominant substrates and specific

binding motifs of SAMHD1, many retroelement RNAs were bound to SAMHD1. My RNA-seq analysis further displayed that in *SAMHD1*-deficient THP-1 cells, many endogenous retroelement RNAs, primarily LINEs and LTR elements, are upregulated significantly. Therefore, the accumulated retroelement-derived RNA transcripts could be direct substrates of SAMHD1, functioning as immunostimulatory RNAs to activate the type I IFN response. The fundamental question that still remains unanswered is which RNA sensors are involved in linking *SAMHD1*-deficiency to an IFN response. In addition, PI3K/AKT plays an important role in multiple signaling pathway and regulating various cellular function (62). AKT performs diverse tasks by controlling numerous downstream effectors. Therefore, downstream effector of AKT which directly activate IRF3 needs to be identified. On the other hand, I also observed that lots of genes are significantly regulated by *SAMHD1*-deficiency in direct or indirect manner and various RNA species, which include small nucleolar RNAs (snoRNAs), are bound to SAMHD1 protein. snoRNAs are known to guide the modification (2'-O-methylation and pseudouridylation) of RNAs represented by rRNAs (63) and the incorporation of 2'-O-methylated nucleosides or pseudouridine into RNA diminishes immunostimulatory activity (64, 65). Therefore, SAMHD1 would indirectly affect the immunostimulatory activity of endogenous RNAs by regulating RNA modification, accounting for a partial role for entire type I IFN response in *SAMHD1*-deficient cells. Considering the phenotypical overlap of

AGS with SLE, the pathology of SLE patients, in some cases, might be associated with the accumulation of aberrantly metabolized endogenous nucleic acids. A greater understanding of the pathogenesis of type I interferonopathies is not only of scientific interest but might lead to new therapies for autoinflammatory diseases.

REFERENCES

1. Hrecka K, *et al.* (2011) Vpx relieves inhibition of HIV-1 infection of macrophages mediated by the SAMHD1 protein. *Nature* **474**(7353):658-661.
2. Laguette N, *et al.* (2011) SAMHD1 is the dendritic- and myeloid-cell-specific HIV-1 restriction factor counteracted by Vpx. *Nature* **474**(7353):654-657.
3. Li N, Zhang W, & Cao X (2000) Identification of human homologue of mouse IFN-gamma induced protein from human dendritic cells. *Immunol Lett* **74**(3):221-224.
4. Qiao F & Bowie JU (2005) The many faces of SAM. *Sci STKE* **2005**(286):re7.
5. Aravind L & Koonin EV (1998) The HD domain defines a new superfamily of metal-dependent phosphohydrolases. *Trends Biochem Sci* **23**(12):469-472.
6. Powell RD, Holland PJ, Hollis T, & Perrino FW (2011) Aicardi-Goutieres syndrome gene and HIV-1 restriction factor SAMHD1 is a dGTP-regulated deoxynucleotide triphosphohydrolase. *J Biol Chem* **286**(51):43596-43600.
7. Goldstone DC, *et al.* (2011) HIV-1 restriction factor SAMHD1 is a deoxynucleoside triphosphate triphosphohydrolase. *Nature* **480**(7377):379-382.
8. Ji X, *et al.* (2013) Mechanism of allosteric activation of SAMHD1 by dGTP. *Nat Struct Mol Biol* **20**(11):1304-1309.
9. Tang C, Ji X, Wu L, & Xiong Y (2015) Impaired dNTPase activity of SAMHD1 by phosphomimetic mutation of Thr-592. *J Biol Chem* **290**(44):26352-26359.
10. Arnold LH, *et al.* (2015) Phospho-dependent Regulation of SAMHD1 Oligomerisation Couples Catalysis and Restriction. *PLoS Pathog* **11**(10):e1005194.
11. Lee EJ, *et al.* (2017) SAMHD1 acetylation enhances its deoxynucleotide triphosphohydrolase activity and promotes cancer cell proliferation. *Oncotarget* **8**(40):68517-68529.
12. Ryoo J, *et al.* (2014) The ribonuclease activity of SAMHD1 is required for HIV-1 restriction. *Nat Med* **20**(8):936-941.
13. Ryoo J, Hwang SY, Choi J, Oh C, & Ahn K (2016) SAMHD1, the Aicardi-Goutieres syndrome gene and retroviral restriction factor, is a phosphorolytic ribonuclease rather than a hydrolytic ribonuclease. *Biochem*

- Biophys Res Commun* **477**(4):977-981.
14. Brandariz-Nunez A, *et al.* (2012) Role of SAMHD1 nuclear localization in restriction of HIV-1 and SIVmac. *Retrovirology* **9**:49.
 15. Hofmann H, *et al.* (2012) The Vpx lentiviral accessory protein targets SAMHD1 for degradation in the nucleus. *J Virol* **86**(23):12552-12560.
 16. Baldauf HM, *et al.* (2012) SAMHD1 restricts HIV-1 infection in resting CD4(+) T cells. *Nat Med* **18**(11):1682-1687.
 17. Diamond TL, *et al.* (2004) Macrophage tropism of HIV-1 depends on efficient cellular dNTP utilization by reverse transcriptase. *J Biol Chem* **279**(49):51545-51553.
 18. Amie SM, Noble E, & Kim B (2013) Intracellular nucleotide levels and the control of retroviral infections. *Virology* **436**(2):247-254.
 19. Skasko M, *et al.* (2005) Mechanistic differences in RNA-dependent DNA polymerization and fidelity between murine leukemia virus and HIV-1 reverse transcriptases. *J Biol Chem* **280**(13):12190-12200.
 20. Banapour B, Marthas ML, Munn RJ, & Luciw PA (1991) In vitro macrophage tropism of pathogenic and nonpathogenic molecular clones of simian immunodeficiency virus (SIVmac). *Virology* **183**(1):12-19.
 21. Gao WY, Cara A, Gallo RC, & Lori F (1993) Low levels of deoxynucleotides in peripheral blood lymphocytes: a strategy to inhibit human immunodeficiency virus type 1 replication. *Proc Natl Acad Sci U S A* **90**(19):8925-8928.
 22. Fujita M, *et al.* (2008) Vpx is critical for reverse transcription of the human immunodeficiency virus type 2 genome in macrophages. *J Virol* **82**(15):7752-7756.
 23. Srivastava S, *et al.* (2008) Lentiviral Vpx accessory factor targets VprBP/DCAF1 substrate adaptor for cullin 4 E3 ubiquitin ligase to enable macrophage infection. *PLoS Pathog* **4**(5):e1000059.
 24. Lahouassa H, *et al.* (2012) SAMHD1 restricts the replication of human immunodeficiency virus type 1 by depleting the intracellular pool of deoxynucleoside triphosphates. *Nat Immunol* **13**(3):223-228.

25. Kim B, Nguyen LA, Daddacha W, & Hollenbaugh JA (2012) Tight interplay among SAMHD1 protein level, cellular dNTP levels, and HIV-1 proviral DNA synthesis kinetics in human primary monocyte-derived macrophages. *J Biol Chem* **287**(26):21570-21574.
26. St Gelais C, *et al.* (2012) SAMHD1 restricts HIV-1 infection in dendritic cells (DCs) by dNTP depletion, but its expression in DCs and primary CD4+ T-lymphocytes cannot be upregulated by interferons. *Retrovirology* **9**:105.
27. White TE, *et al.* (2013) The Retroviral Restriction Ability of SAMHD1, but Not Its Deoxynucleotide Triphosphohydrolase Activity, Is Regulated by Phosphorylation. *Cell Host Microbe* **13**(4):441-451.
28. Cribier A, Descours B, Valadao ALC, Laguette N, & Benkirane M (2013) Phosphorylation of SAMHD1 by Cyclin A2/CDK1 Regulates Its Restriction Activity toward HIV-1. *Cell Reports* **3**(4):1036-1043.
29. Beloglazova N, *et al.* (2013) Nuclease activity of the human SAMHD1 protein implicated in the Aicardi-Goutieres syndrome and HIV-1 restriction. *J Biol Chem* **288**(12):8101-8110.
30. Seamon KJ, Sun Z, Shlyakhtenko LS, Lyubchenko YL, & Stivers JT (2015) SAMHD1 is a single-stranded nucleic acid binding protein with no active site-associated nuclease activity. *Nucleic Acids Res* **43**(13):6486-6499.
31. Welbourn S & Strebel K (2016) Low dNTP levels are necessary but may not be sufficient for lentiviral restriction by SAMHD1. *Virology* **488**:271-277.
32. Rice GI, *et al.* (2009) Mutations involved in Aicardi-Goutieres syndrome implicate SAMHD1 as regulator of the innate immune response. *Nat Genet* **41**(7):829-832.
33. Crow YJ & Manel N (2015) Aicardi-Goutieres syndrome and the type I interferonopathies. *Nat Rev Immunol* **15**(7):429-440.
34. Crow YJ, *et al.* (2006) Mutations in the gene encoding the 3'-5' DNA exonuclease TREX1 cause Aicardi-Goutieres syndrome at the AGS1 locus. *Nat Genet* **38**(8):917-920.
35. Crow YJ, *et al.* (2015) Characterization of human disease phenotypes associated with mutations in TREX1, RNASEH2A, RNASEH2B, RNASEH2C,

- SAMHD1, ADAR, and IFIH1. *Am J Med Genet A* **167A**(2):296-312.
36. Rice GI, *et al.* (2012) Mutations in ADAR1 cause Aicardi-Goutieres syndrome associated with a type I interferon signature. *Nat Genet* **44**(11):1243-1248.
 37. Rice GI, *et al.* (2014) Gain-of-function mutations in IFIH1 cause a spectrum of human disease phenotypes associated with upregulated type I interferon signaling. *Nat Genet* **46**(5):503-509.
 38. Oda H, *et al.* (2014) Aicardi-Goutieres syndrome is caused by IFIH1 mutations. *Am J Hum Genet* **95**(1):121-125.
 39. Kim S, *et al.* (2015) Temporal Landscape of MicroRNA-Mediated Host-Virus Crosstalk during Productive Human Cytomegalovirus Infection. *Cell Host Microbe* **17**(6):838-851.
 40. Li B & Dewey CN (2011) RSEM: accurate transcript quantification from RNA-Seq data with or without a reference genome. *BMC Bioinformatics* **12**:323.
 41. Ritchie ME, *et al.* (2015) limma powers differential expression analyses for RNA-sequencing and microarray studies. *Nucleic Acids Res* **43**(7):e47.
 42. Behrendt R, *et al.* (2013) Mouse SAMHD1 has antiretroviral activity and suppresses a spontaneous cell-intrinsic antiviral response. *Cell Rep* **4**(4):689-696.
 43. Rehwinkel J, *et al.* (2013) SAMHD1-dependent retroviral control and escape in mice. *EMBO J* **32**(18):2454-2462.
 44. Lim YW, Sanz LA, Xu X, Hartono SR, & Chedin F (2015) Genome-wide DNA hypomethylation and RNA:DNA hybrid accumulation in Aicardi-Goutieres syndrome. *Elife* **4**.
 45. Kretschmer S, *et al.* (2015) SAMHD1 prevents autoimmunity by maintaining genome stability. *Ann Rheum Dis* **74**(3):e17.
 46. Chen Q & Ross AC (2004) Retinoic acid regulates cell cycle progression and cell differentiation in human monocytic THP-1 cells. *Exp Cell Res* **297**(1):68-81.
 47. Martinez FO, Gordon S, Locati M, & Mantovani A (2006) Transcriptional profiling of the human monocyte-to-macrophage differentiation and polarization: new molecules and patterns of gene expression. *Journal of*

- immunology* **177**(10):7303-7311.
48. Johnston JB, *et al.* (2001) Monocyte activation and differentiation augment human endogenous retrovirus expression: implications for inflammatory brain diseases. *Ann Neurol* **50**(4):434-442.
 49. Alexopoulou L, Holt AC, Medzhitov R, & Flavell RA (2001) Recognition of double-stranded RNA and activation of NF-kappaB by Toll-like receptor 3. *Nature* **413**(6857):732-738.
 50. Diebold SS, Kaisho T, Hemmi H, Akira S, & Reis e Sousa C (2004) Innate antiviral responses by means of TLR7-mediated recognition of single-stranded RNA. *Science* **303**(5663):1529-1531.
 51. Heil F, *et al.* (2004) Species-specific recognition of single-stranded RNA via toll-like receptor 7 and 8. *Science* **303**(5663):1526-1529.
 52. Kato H, *et al.* (2006) Differential roles of MDA5 and RIG-I helicases in the recognition of RNA viruses. *Nature* **441**(7089):101-105.
 53. Darnell JE, Jr., Kerr IM, & Stark GR (1994) Jak-STAT pathways and transcriptional activation in response to IFNs and other extracellular signaling proteins. *Science* **264**(5164):1415-1421.
 54. Plataniotis LC (2005) Mechanisms of type-I- and type-II-interferon-mediated signalling. *Nat Rev Immunol* **5**(5):375-386.
 55. Wang H, *et al.* (2008) IFN-beta production by TLR4-stimulated innate immune cells is negatively regulated by GSK3-beta. *J Immunol* **181**(10):6797-6802.
 56. Choi J, Ryoo J, Oh C, Hwang S, & Ahn K (2015) SAMHD1 specifically restricts retroviruses through its RNase activity. *Retrovirology* **12**:46.
 57. Goncalves A, *et al.* (2012) SAMHD1 is a nucleic-acid binding protein that is mislocalized due to aicardi-goutieres syndrome-associated mutations. *Hum Mutat* **33**(7):1116-1122.
 58. Maksakova IA, *et al.* (2006) Retroviral elements and their hosts: insertional mutagenesis in the mouse germ line. *PLoS Genet* **2**(1):e2.
 59. Goke J, *et al.* (2015) Dynamic transcription of distinct classes of endogenous retroviral elements marks specific populations of early human embryonic

- cells. *Cell Stem Cell* **16**(2):135-141.
60. Maelfait J, Bridgeman A, Benlahrech A, Cursi C, & Rehwinkel J (2016) Restriction by SAMHD1 Limits cGAS/STING-Dependent Innate and Adaptive Immune Responses to HIV-1. *Cell Rep* **16**(6):1492-1501.
 61. Lander ES, *et al.* (2001) Initial sequencing and analysis of the human genome. *Nature* **409**(6822):860-921.
 62. Nitulescu GM, *et al.* (2016) Akt inhibitors in cancer treatment: The long journey from drug discovery to clinical use (Review). *Int J Oncol* **48**(3):869-885.
 63. Scott MS & Ono M (2011) From snoRNA to miRNA: Dual function regulatory non-coding RNAs. *Biochimie* **93**(11):1987-1992.
 64. Jockel S, *et al.* (2012) The 2'-O-methylation status of a single guanosine controls transfer RNA-mediated Toll-like receptor 7 activation or inhibition. *J Exp Med* **209**(2):235-241.
 65. Kariko K, Buckstein M, Ni H, & Weissman D (2005) Suppression of RNA recognition by Toll-like receptors: the impact of nucleoside modification and the evolutionary origin of RNA. *Immunity* **23**(2):165-175.

ABSTRACT IN KOREAN

SAMHD1은 dNTPase와 RNase, 두 가지 효소 활성을 가지고 있는 단백질이다. SAMHD1은 마우스의 Mg11 유전자의 이중상동성 유전자로 알려졌다. 대부분의 연구가 HIV-1 조절 기작과 관련되어서 진행되어왔다. SAMHD1은 초기에 역전사에 필요한 dNTP를 분해함으로써 HIV-1의 복제를 억제하는 것으로 알려졌다. 이후 직접 HIV-1 RNA와 결합하고 분해함으로써 이를 조절하는 경로 또한 보고되었다.

제 1형 인터페론 신호전달 과정의 항상성이 무너지게 되면 자가면역질환이 생성될 수 있다. AGS는 지속적인 제 1형 인터페론 신호전달과정의 활성화를 특징으로 가지는 자가면역질환의 하나로 선천적인 바이러스 감염이나 전신성 홍반성 루프스와 유사한 병증을 보이는 것으로 알려져 있다. AGS 환자에게서 돌연변이가 일어나는 것으로 알려져 있는 원인 유전자들은 대부분 핵산 대사 과정과 연관되어 있기 때문에, 대사 과정에서 적절하게 처리되지 못한 핵산들이 세포 내부에 축적되고 나아가 지속적인 제 1형 인터페론 생성을 유도하는 것으로 추측되고 있다. TREX1, RNASEH2, ADAR1 그리고 IFIH1과 같은 단백질의 기능 이상으로 생겨나는 AGS에 대해서는 상대적으로 연구가 많이 되었고, 그 작용 기작도 어느정도 보고된 바 있다. 하지만 SAMHD1의 유전적 결손을 가진 AGS 환자에게서 발생하고 있는 지속적인 제 1형 인터페론 반응이 어떠한 메커니즘을 통해서 유도되는지는 아직까지 정확하게 밝혀지지 않았다.

이 연구에서 나는 SAMHD1이 결손된 사람 단핵 백혈구 세포를 만들었고, 이 세포에서 AGS와 같은 제 1형 인터페론 반응이 나타나는 것을 관찰하였다. 사람 단핵 백혈구 세포에 존재하는 SAMHD1은 RNase 효소 활성을 가지고 있었고, SAMHD1이 결손된 세포에서 추출한 핵산 중 RNA에 의해서만 WT에서 추출한 핵산과 달리 유의미한 제 1형 인터페론 반응이 나타나는 것을 확인할 수 있었다. 또한 SAMHD1이 결손된 세포에 야생형 SAMHD1과 dNTPase 혹은 RNase로서의 기능이 각각 손상된 혹은 두 가지 효소 기능이 모두 상실된 돌연변이 SAMHD1을 재구축해 봄으로써, SAMHD1의 RNA 분해 효소 기능이 제 1형 인터페론 반응을 완화 시키는데 중요하게 작용한다는 것을 확인할 수 있었다. 이 결과는 정상적인 상황에서 SAMHD1에 의해 조절되는 내재적인 RNA 기질들이 SAMHD1이 결손됨에 따라 분해되지 못하고 세포 내부에 축적되고, 이 RNA를 면역 반응의 기질로 이용하는 제 1형 인터페론 반응이 활성화 된다는 것을 시사한다. 또한, RNA-seq과 SAMHD1-CLIP seq 데이터 분석을 통해 내재적 레트로엘레먼트에 의해서 전사된 RNA가 SAMHD1 결손에 의한 AGS를 유도하는 주요한 원인물질이 될 수 있다는 것을 예상할 수 있었다. 이러한 제 1형 인터페론 반응은 기존에 핵산 매개 반응에서 중요한 역할을 하는 것으로 잘 알려진 단백질인 TBK1에 의해서 영향을 받지 않고, 오직 IRF3의 의해서만 조절되는 것을 확인할 수 있었다. 이러한 사실을 바탕으로 하여 나는 SAMHD1의

결손에 의해 나타나는 제 1형 인터페론 반응은 기존에 잘 보고된 RNA 매개 선천성 면역 반응 경로가 아니라 PI3K/AKT/IRF3를 축으로 하는 새로운 RNA 인지 경로를 통해서 유도된다는 것을 밝혔다. AKT와 IRF3는 SAMHD1이 결손된 세포에서 강하게 인산화됨으로써 그 기능이 활성화되어 있었다. PI3K나 AKT 단백질에 대한 억제제를 SAMHD1이 결손된 세포에 처리하였을 경우 제 1형 인터페론 반응의 활성이 눈에 띄게 저해된다는 사실을 관찰할 수 있었다. 또한 유전자 조작 기술을 이용하여 SAMHD1이 결손된 세포에서 AKT를 추가로 결손 시키거나 siRNA를 이용하여 IRF3를 결핍시켰을 경우에도 억제제 처리시와 동일하게 인터페론 반응이 감소되는 것을 확인하였다. 이러한 AKT의 활성 또한 제 1형 인터페론 반응과 마찬가지로 SAMHD1의 RNase 효소 기능에 의해서 조절된다는 사실을 SAMHD1 재구축실험을 통해서 밝혀낼 수 있었다. 사람 단핵 백혈구 세포뿐만 아니라 말초 혈액 단핵구 세포에서도 SAMHD1 결핍에 의한 제 1형 인터페론 반응이 유도되는 것을 확인하였으나, HEK293T나 HeLa 세포에서는 이러한 결과가 나타나지 않았다. 이를 통해서 SAMHD1 결손에 의해 나타나는 제 1형 인터페론 반응이 세포 특이적인 현상이라는 것을 확인할 수 있었다. 본 연구를 통해서 새로이 밝혀낸 AGS 관련 RNA 인지 신호전달 경로는 AGS나 그와 유사한 자가면역질환에 대한 분자생물학적 발생기전 연구에 새로운 방향성을 제시할 뿐만 아니라 새로운 치료제 개발의 단초가 될 것으로 기대된다.

주요검색어: AGS, SAMHD1, RNA 분해효소, PI3K, AKT, IRF3,

자가면역질환

학번: 2009-30842

APPENDIX

Educational background

2000-2007 B.S.

Department of Biology Education, College of Education, Seoul National University

2007-2009 M.S.

Department of Interdisciplinary Program in Genetic Engineering, College of Natural Science, Seoul National University

2009-present Ph.D.course

Department of Interdisciplinary Program in Genetic Engineering, College of Natural Science, Seoul National University

Publications

Oh C, Ryoo J, Park K, Kim B, Daly M, Cho D and Ahn K. A central role for PI3K-AKT signaling pathway in linking *SAMHD1*-deficiency to the type I interferon signature. *Scientific Reports*. 2018 Jan 8;8(1):84.

Ryoo J, Hwang S-Y, Choi J, **Oh C** and Ahn K. Correspondence. *Nat Med*. 2016 Oct 6;22(10):1074-1075.

Ryoo J, Hwang S-Y, Choi J, **Oh C** and Ahn K. *SAMHD1*, The Aicardi-Goutieres syndrome gene and retroviral restriction factor, is a phosphorolytic

ribonuclease rather than a hydrolytic ribonuclease. *Biochem Biophys Res Commun.* 2016 Sep 2;477(4):977-981.

Choi J, Ryoo J, **Oh C**, Hwang S and Ahn K. SAMHD1 specifically restricts retroviruses through its RNase activity. *Retrovirology.* 2015 Jun 2;12:46.

Ryoo J, Choi J, **Oh C**, Kim S, Seo M, Kim S, Seo D, Kim J, White TE, Brandariz-Nunez A, Diaz-Griffero F, Yun CH, Hollenbaugh JA, Kim B, Baek D and Ahn K. The ribonuclease activity of SAMHD1 is required for HIV-1 restriction. *Nat Med.* 2014 Aug;20(8):936-41.

Cho K, Cho S, Lee SO, **Oh C**, Kang K, Ryoo J, Lee S, Kang S and Ahn K. Redox-regulated peptide transfer from the transporter associated with antigen processing to major histocompatibility complex class I molecules by protein disulfide isomerase. *Antioxid Redox Signal.* 2011 Aug 1;15(3):621-33.

Lee SO, Cho K, Cho S, Kim I, **Oh C** and Ahn K. Protein disulphide isomerase is required for signal peptide peptidase-mediated protein degradation. *EMBO J.* 2010 Jan 20;29(2):363-75.

Kang K, Park B, **Oh C**, Cho K and Ahn K. A role for protein disulfide isomerase in the early folding and assembly of MHC class I molecules. *Antioxid Redox Signal.* 2009 Oct;11(10):2553-61.

Kim Y, Kang K, Kim I, Lee YJ, **Oh C**, Ryoo J, Jeong E and Ahn K. Molecular mechanisms of MHC class I-antigen processing: redox considerations. *Antioxid Redox Signal.* 2009 Apr;11(4):907-36.